Design and Analysis of Wideband DRA

A Thesis submitted in partial fulfillment of the Requirements for the degree of

Master of Technology

in

Communication and Networks

by

Manish Pradhan

Roll No: 212EC5175

Department of Electronics and Communication Engineering

National Institute of Technology Rourkela

Rourkela, Odisha, 769008

May 2014

Design and Analysis of Wideband DRA

A Thesis submitted in partial fulfillment of the Requirements for the degree of

Master of Technology

in

Communication and Networks

by

Manish Pradhan

Roll No: 212EC5175

Under the Guidance of

Prof. Santanu Kumar Behera

Department of Electronics and Communication Engineering

National Institute of Technology Rourkela

Rourkela, Odisha, 769008

May 2014

DEPARTMENT OF ELECTRONICS AND COMMUNICATION ENGINEERING

NATIONAL INSTITUTE OF TECHNOLOGY, ROURKELA

ROURKELA- 769008, ODISHA, INDIA

CERTIFICATE

This is to certify that the work in this thesis entitled "**DESIGN AND ANALYSIS OF WIDEBAND DRA"** by Mr. **MANISH PRADHAN** is a record of an original research work carried out by him during 2013-2014 under my supervision and guidance in partial fulfilment of the requirement for the award of the degree of Master of Technology in Electronics and Communication Engineering (Communication and Networks), National Institute of Technology, Rourkela. Neither this thesis nor any part of it, to the best of my knowledge, has been submitted for any degree or diploma elsewhere.

Place: NIT Rourkela

Date: 27th May 2014

Prof. Santanu Kumar Behera

Associate Professor

DEPARTMENT OF ELECTRONICS AND COMMUNICATION ENGINEERING

NATIONAL INSTITUTE OF TECHNOLOGY, ROURKELA

ROURKELA- 769008, ODISHA, INDIA

Declaration

I certify that

a) The work comprised in the thesis is original and is done by myself under the supervision of my supervisor.

b) The work has not been submitted to any other institute for any degree or diploma.

c) I have followed the guidelines provided by the Institute in writing the thesis.

d) Whenever I have used materials (data, theoretical analysis, and text) from other sources, I have given due credit to them in the text of the thesis and giving their details in the references.

e) Whenever I have quoted written materials from other sources, I have put them under quotation marks and given due credit to the sources by citing them and giving required details in the references.

Manish Pradhan

212EC5175

Acknowledgements

The work posed in this thesis is by far the most substantial attainment in my life and it would be unimaginable without people who affirmed me and believed in me. First and foremost I evince my profound reverence and deep regards to my guide Prof. S. K. Behera for exemplary guidance, supervising and constant encouragement throughout the course of this thesis. A gentleman embodied, in true form and spirit, I consider it to my good fortune to have consociated with him.

I would like to evince a deep sense of gratitude to estimable Prof. S. Meher, Head of the Department of Electronics and Communication Engineering for providing us with best facilities and his timely suggestions.

My special thanks to Prof. S K. Patra, Prof. K. K. Mahapatra of Department of Electronics and Communication Engineering for their constant inspiration and encouragement during my research. I want to thank all other faculty members of Department of Electronics and Communication Engineering for their constant support and encouragement during my research. My special thanks to Ph.D scholars Runa Kumari, Yogesh Kumar Choukiker, Natarajamani S, Ayashkanta Panigrahi for their help, cooperation and encouragement. I would like to thank all my friends who made my journey at NIT Rourkela an indelible and gratifying experience.

Finally, my heartfelt gratitude towards my family for their tireless love and support throughout my life. They taught me the value of hard work by their own life example. They gave me tremendous support during my stay in NIT Rourkela.

Manish Pradhan

Abstract

The thesis gives a sense of the freedom provided by dielectric resonator antennas (DRAs) and their possible advantages compared to the traditional low-gain antennas like monopole and patch antenna. At first the thesis covers the analysis on simple shaped DRA like hemispherical, cylindrical and rectangular, and presents the design equations for predicting the resonant frequency and radiation Q-factor. A brief review of coupling theory and more common feeding methods are then surveyed. Various bandwidth enhancement techniques like the reduction of Q-factor by loading effect, modification in feeding element and DRA shapes, multiple DRAs, and hybrid antennas are also covered. In the end, using few of the above techniques, three wide band (Impedance Bandwidth above 20%) antennas based on rectangular and cylindrical shapes, one operating in C-band (4 – 8 GHz) and the other two in X-band (8 – 12 GHz) are designed and simulated on CST Microwave Studio.

Table of Contents

List of Figures

List of Tables

Chapter 1

Introduction

The field of wireless communications has been growing since the invention of portable mobile phones some 25 years ago. The success of the second-generation (2G) cellular communication services leads to the development of wideband third-generation (3G) and fourth-generation (4G) cellular phones and other wireless products and services, including wireless LAN, Bluetooth etc. The devices using these communication services are mostly portable and run on batteries. That means, components in these devices should be of small size and consume low power. Moreover, some wireless devices are required to support multiple wireless services and very high data rate. As an antenna is the crucial part of any wireless device, the development of highly efficient, low-profile, small-size, multi-band and wide band antennas that can be made embedded into wireless products are very much demanded.

In the last 3 decades, two classes of antennas have been extensively investigated. They are the microstrip patch antenna and the dielectric resonator antenna (DRA). Both are highly suitable for the development of modern wireless communications.

Microstrip antennas have many advantages. They have a very low profile, are mechanically rugged and are inexpensive to fabricate. But they have disadvantages like narrow bandwidth, surface wave loss, low gain and low efficiency. Moreover, as the frequency increases toward millimetre wavelengths, the conduction losses become severe resulting in very poor efficiency.

DRA lack metal parts that results in zero conduction loss. It has much wider impedance bandwidth as compared to the patch antenna. Moreover, a high-permittivity dielectric resonator can be used as a small and low-profile antenna operated at lower microwave frequencies. The above mentioned characteristics of DRA can be employed in some compact portable wireless devices, military millimetre-wave radar equipment and satellite communication.

`

1.2 Thesis Objective

The objective of this thesis is to study the working principle of the Dielectric Resonator antenna (DRA) and to confirm the validity of the design equations and the capability of DRA. It includes the design of DRA with the required resonant frequency and impedance bandwidth. Comparison of DRA and microstrip antenna is also one of the objectives. As the basic DRA like rectangular and cylindrical do not satisfy the requirement of very high bandwidth and high gain, the objective includes the methods to enhance the bandwidth of basic DRA.

1.3 Thesis Outline

The purpose of this thesis is to give an understanding of the fundamental operation of DRAs and to give an overview of the various aspects of DRA technology, emphasizing design and simulation.

Chapter 2 introduces DRA with an historical review, characteristics and limitations. Chapters 3 and 4 deal with the fundamentals of DRAs. Chapter 3 introduces the basic and most commonly used shapes (hemispherical, cylindrical, and rectangular) of the DRA. For each of these shapes, the fundamental modes of operation are described and design equations are provided for determining the resonant frequency and radiation Q-factor of an isolated DRA. Design examples are also shown to illustrate the performance of these simple shaped DRAs. Chapter 4 then focuses on the various coupling methods that have been used to excite DRAs. Chapter 5 discusses the theoretical bandwidth behaviour of simple shaped DRAs and then looks at the various methods for improving the impedance bandwidth.

Chapter 6 and 7 covers the design part of the thesis. Chapter 6 looks at the design of aperture coupled hemispherical DRA resonating at desired resonant frequency of 5.2 GHZ and 8% impedance bandwidth. Chapter 7 focuses on wide band DRA design using bandwidth enhancement techniques of the chapter 5. It contains two designs. One is DRA-loaded microstrip antenna working in C-band (4 GHz-8 GHz) and the other is flipped staired pyramid and conical DRA working in X-band (8 GHz-12 GHz)

Chapter 8 concludes the thesis.

Chapter 2

Introduction to Dielectric Resonator Antennas

Dielectric Resonator Antennas (DRAs) are dielectric resonators (DR) that radiate energy into space when excited appropriately. It consists of a piece of ceramic material of various shapes having high dielectric constant. It is placed on a metal surface and feeding circuit is used to introduce EM waves inside it which bounce back and forth between the walls of the resonator that forms standing waves. The walls of the resonator are partially transparent to EM waves that allow the EM power to radiate into space.

The resonant frequency of DRA is determined by the shape of the block, overall physical dimensions, and the dielectric constant of the material. The resonance is similar to that of a hollow metallic waveguide cavity, except that the boundary is defined by large change in permittivity rather than by a conductor.

2.1 Historical review

Metal Waveguide cavities of simple shapes like rectangular, cylindrical etc. have been analysed for a long time as a special case of waveguides. There exist explicit expressions for calculating the resonant frequencies and electromagnetic fields in such resonant cavity. In 1939, Stanford University showed that dielectric objects shaped like toroids could also be used as microwave resonators [1]. This is where the term dielectric resonator (DR) first appeared. Their modes were first analysed in the early 1960s [2]. Initially, for many years, the DR is used as high-Q elements for circuit applications, such as filters and oscillators, offering a more compact alternative to the waveguide cavity resonator and a more amenable technology for printed circuit integration [3, 4]. For these applications, The DRs are usually shielded to prevent radiation and thus to maintain a high Q-factor, required for oscillator and filter designs.

If the shielding is removed and with the proper excitation to launch the appropriate mode, these same dielectric resonators can actually become efficient radiators. Furthermore, by lowering the dielectric constant, the radiation can be maintained over a

relatively broad band of frequencies. The study of dielectric resonators as radiating elements began in the 1980s with the examination of the characteristics of cylindrical, rectangular and hemispherical shape by Long, McAllister, and Shen [5-7]. Analysis of their resonant modes, radiation patterns, and methods of excitation made it clear that these DR could be used as antennas and offered a new and attractive alternative to traditional low gain antennas. These decade also saw a demonstration of the first linear arrays of DRAs and the first planar array.

In the early 1990s, emphasis was placed on realizing various feeding methods to excite DRAs and on applying various analytic or numerical techniques for determining the input impedance and Q-factor. Much of the early work to characterize the performance of the basic DRA elements is summarized in a 1994 review paper by Mongia and Bhartia [8], which also proposed to standardize the mode nomenclature and provided a set of simple equations for predicting the resonant frequency and Q-factors for several DRA shapes.

By the mid-1990s more attention was being given to linear and planar arrays of DRAs. This period also saw the development of low-profile and compact designs, mutual-coupling analysis of array elements, circular-polarized DRAs, multi-band/wideband designs, active/tunable DRAs, and the beginnings of hybrid antenna designs.

Since the start of the new millennium, more researchers have entered the field of DRA. Emphasis has on compact designs to address the needs of portable wireless applications and on new DRA shapes or hybrid antennas for enhanced bandwidth performance to meet the requirements for emerging broadband or ultra wideband systems.

2.2 Characteristics of the dielectric resonator antennas

1) High radiation efficiency: At high microwave and millimetre wave frequencies, the conductor loss of metallic antennas becomes intense and the efficiency of the antennas is reduced significantly. An advantage of DRA is they lack metal parts. So DRA can be more efficient than metal antennas at these frequencies.

2) Small size: The size of the DRA is proportional to $\lambda_0 / \sqrt{\varepsilon_r}$, where λ_0 is the free space wavelength at the resonant frequency and ε_r is the dielectric constant of the dielectric resonator. Thus, by using a material with high ε_r, the size of the DRA can be reduced significantly, making it suitable for low–frequency operation.

3) Low-Profile and Compact Designs: DRA provides one or more degree of freedom while designing i.e. for a fixed dielectric constant and shape, it gives many design options of different size all having same resonant frequency. However, the Q-factor will be different.

4) Wide impedance bandwidth: The DRA has a much wider impedance bandwidth as compared to the microstrip antenna. This is because the microstrip antenna radiates only through two narrow radiation slots, whereas the DRA radiates through the whole DRA surface except the grounded part.

5) Radiation pattern: Several modes can be excited within the DRA, many of which has radiation patterns similar to short electric or magnetic dipoles, producing either omnidirectional or broadside radiation patterns.

6) High Gain: DRA operating at their fundamental modes radiate like a short magnetic or electric dipoles. When placed on ground planes, they generate radiation patterns with a maximum directivity of about 5 dBi. For applications requiring higher gain, arrays of DRAs can be used. For medium-gain applications, many techniques are there to increase the directivity of DRA. Gains from 6.3 dBi to 7.8 dBi have been achieved using such techniques.

7) Simple coupling schemes: All excitation methods applicable to the microstrip antenna can be used for the DRA. Probes, slots, microstrip lines, dielectric image guides and coplanar waveguide lines can be used to excite the DRAs efficiently.

8) High power handling capacity: Dielectric resonator antennas have high dielectric strength which makes them capable to handle high power. It can also work in a wide temperature range due to the temperature-stable ceramic materials.

2.3 Limitations

1) Ceramic materials are typically used, which must either be machined from large blocks or cast from moulds. Drilling may be required and the DRA has to be bonded to a ground plane or substrate.

2) Compared to the printed circuit antennas, the fabrication is generally more complex and more costly, especially for array applications.

3) Difficult to get dielectric materials of desired dielectric constants, so have to work with limited available sources.

Chapter 3

Simple Shaped Dielectric Resonator Antennas

This chapter looks at the fundamental modes of three basic DRAs: hemispherical, cylindrical, and rectangular. It also provides design equations and graphs for estimating their resonant frequencies and radiation Q-factors. These designs, however, do not account for the coupling methods used to excite the DRAs, which will load the antenna to some extent. The design equations and curves in this chapter can be used as good starting points for making initial designs.

3.1 The Hemispherical DRA

The geometry of the hemispherical DRA is shown in figure (3.1). It consists of a material with a dielectric constant of ε_r and a radius 'a'. As with all DRA considered in this thesis, the DRA is mounted on a ground plane that is assumed to have infinite conductivity and infinite in extent.

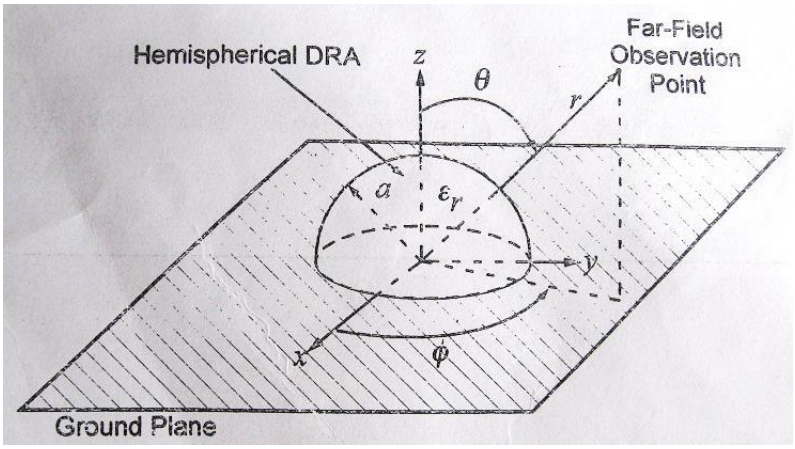

Figure 3. 1: Hemispherical DRA

The modes in a hemispherical DRA can be divided into transverse electric (TE) and transverse magnetic (TM) modes.

3.1.1 The TE_{111} Mode

It is the lowest order mode of the hemispherical DRA. This mode produces a far field radiation pattern similar to that of a short horizontal magnetic dipole, having a wide beam with a broadside peak as shown in figure (3.2). The resonant frequency and radiation Q-factor for this mode can be determined by solving the following characteristic equations:

$$\frac{J_{.5}(\sqrt{\varepsilon_r}\ k_o a)}{J_{1.5}(\sqrt{\varepsilon_r}\ k_o a)} = \frac{H_{.5}^{(2)}(k_o a)}{\sqrt{\varepsilon_r}\, H_{1.5}^{(2)}(k_o a)} \qquad (3.1)$$

Where J(x) is the first order Bessel function, $H^{(2)}(x)$ is the second order Hankel function, and k_o is the free space wave number. The above transcendental eq. is solved to get k_o which is complex.

Resonant frequency, $$f_{GHz} = \frac{4.7713\ Re(k_o a)}{a_{cm}} \qquad (3.2)$$

and $$Q = \frac{4.7713\ Re(k_o a)}{2\ Im(k_o a)} \qquad (3.3)$$

The radiation Q-factor can be used to estimate the fractional impedance bandwidth of an antenna using:

$$BW = \frac{\Delta f}{f_0} = \frac{s-1}{\sqrt{s}\,Q}\ , \qquad (3.4)$$

where Δf is the absolute bandwidth, f_0 is the resonant frequency, and 's' is the maximum acceptable VSWR

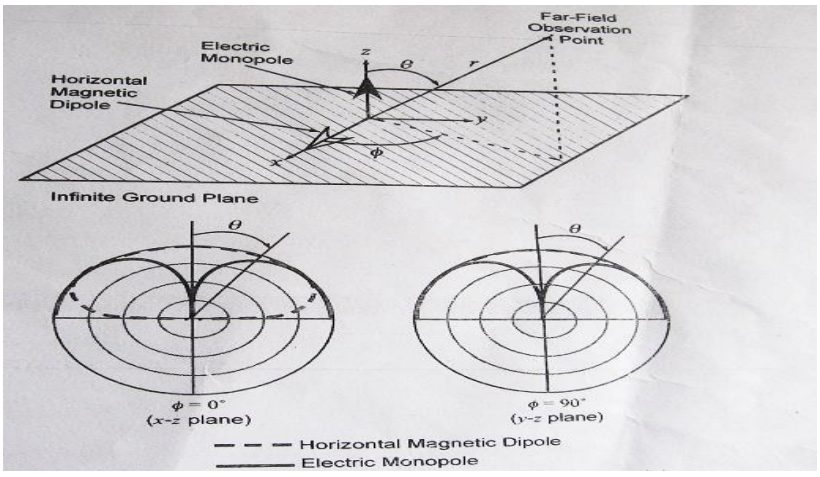

Figure 3. 2: Ideal radiation model of DRA on an infinite ground plane

The $\boldsymbol{Re(\ k_o a)}$ and the Q-factor are plotted as a function of ε_r in figure (3.3) below:

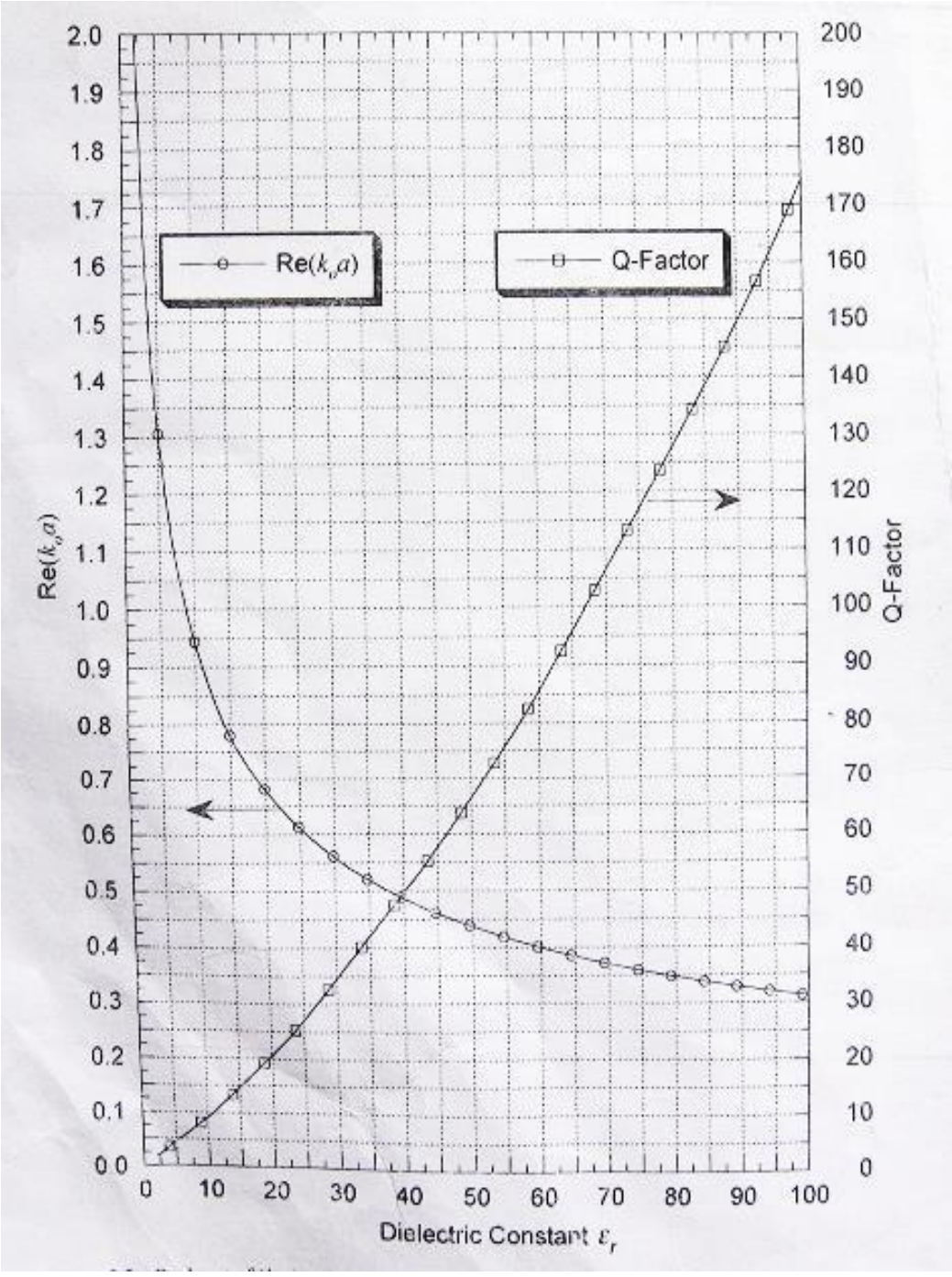

Figure 3. 3: Design curve for TE_{111} mode hemispherical DRA

3.1.2 The TM_{101} Mode

This mode radiates like a short electrical monopole antenna and is typically excited using a probe located at the centre of the DRA (at r = 0). Similar to TE111 mode, it also has transcendental eq. to get resonant frequency and radiation Q-factor.

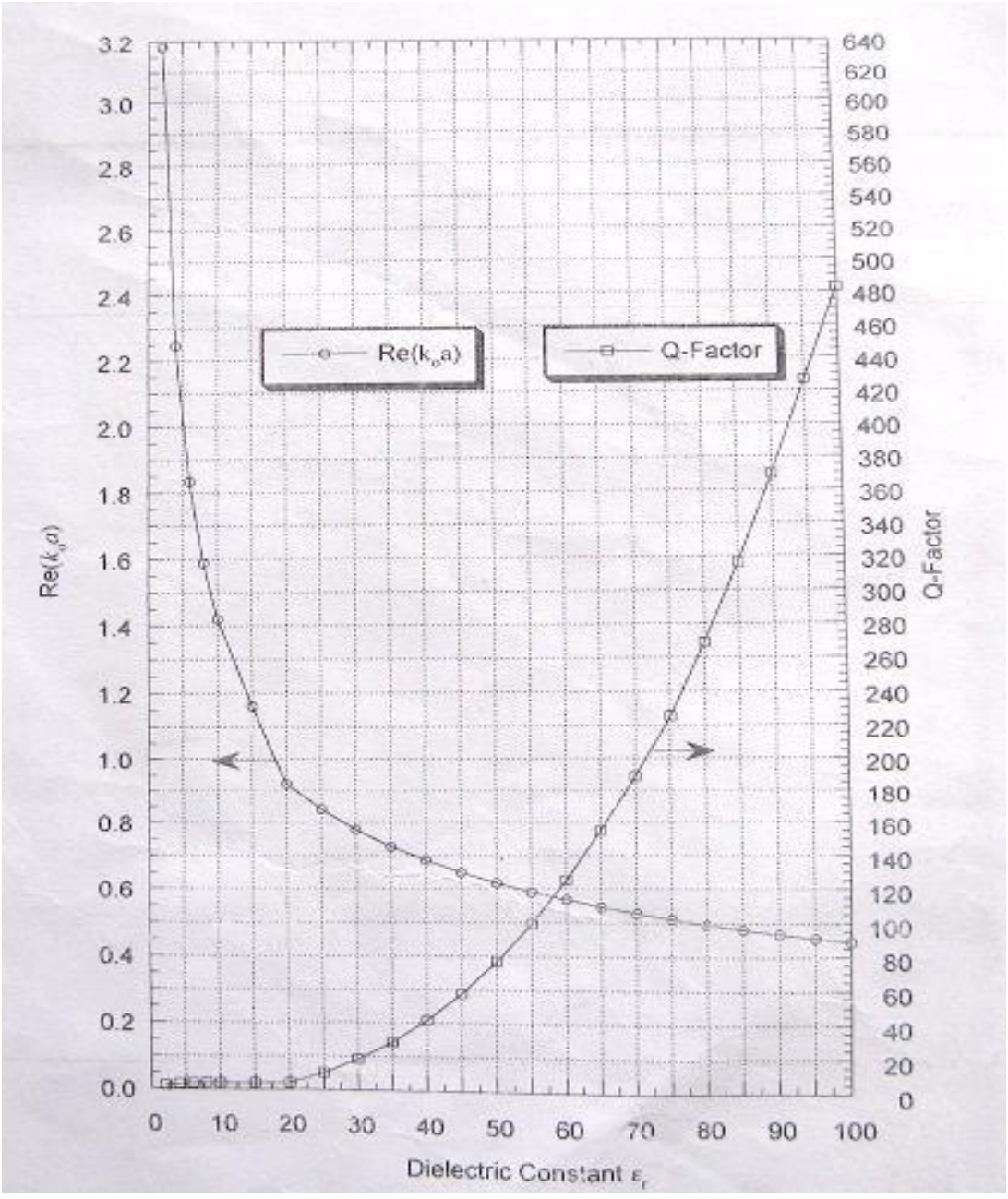

Figure 3. 4: Design curve for TM_{101} mode of the hemispherical resonator antenna

3.1.3 Hemispherical DRA Design Example (TE_{111} Mode)

Determine the radius and dielectric constant of a hemispherical DRA with a resonant frequency of 5.5 GHz and a minimum 8% fractional impedance bandwidth for a VSWR = 2. The solution can be found by the following steps.

Step 1.Determine the Q-factor.

from (3.4), with s = 2, and BW = 0.08, we get Q = 8.84.

Step 2 Determine the dielectric constant.

from Fig 3.3, the value of ε_r for which Q = 8.84 is 10.

Step 3 Determine $Re(\ k_o a)$

from Fig 3.3, the value of $Re(\ k_o a)$ at ε_r = 10 is found to be 0.95.

Step 4 Determine radius.

The radius of the hemispherical DRA is then found using (3.2), where with f_{GHz} = 5.5 and Re(k_oa) = .95, then a = 0.82 cm.

3.2 The Cylindrical DRA

The cylindrical DRA is characterized by a height *h*. a radius *a*, and a dielectric constant ε_r , as shown in figure 3.5

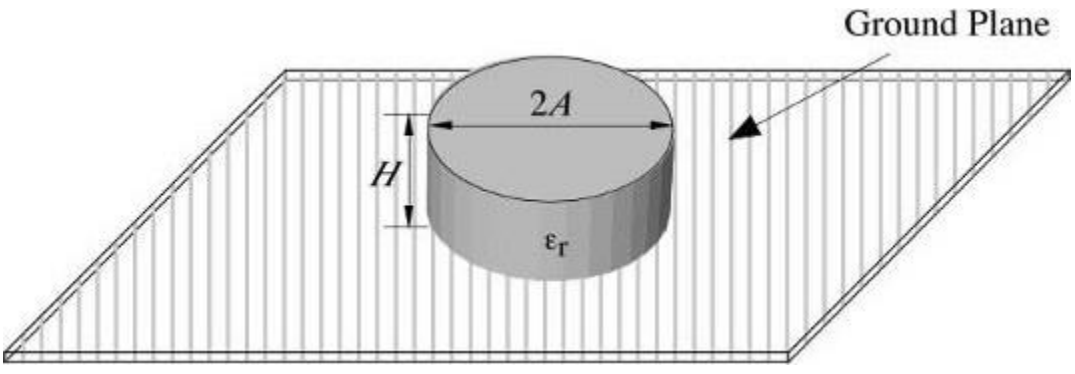

Figure 3. 5: Cylindrical DRA

The cylindrical shape offers one degree of freedom i.e. the aspect ratio *a/h,* which determines $k_o a$ and the Q-factor for a given dielectric constant. Thus a tall, slender cylindrical DRA can

be made to resonate at the same frequency as the wide, thin DRA. However, the Q-factors for these resonators will be different.

3.2.1 Resonant Frequency and Radiation Q-factor

The modes of an isolated cylindrical DRA can be divided into three types: TE, TM, and hybrid modes (called *HE* if the E_z component is dominant, or *EH* if the H_z component is dominant). The modes which are commonly used for radiating applications are the $TM_{01\delta}$, $TE_{01\delta}$, and $HE_{11\delta}$ modes. The $TM_{01\delta}$ mode radiates like a short electric monopole, while the $TE_{01\delta}$ mode radiates like a short magnetic monopole. The $HE_{11\delta}$ mode radiates like a short horizontal magnetic dipole.

The resonant frequency of the *npm* mode:

$$f_{npm} = \frac{1}{2\pi a\sqrt{\mu\varepsilon}}\sqrt{\begin{Bmatrix} X_{np}{}^2 \\ X'_{np}{}^2 \end{Bmatrix} + \left[\frac{\pi a}{2h}\,(2m+1)\right]^2} \qquad (3.5)$$

It is found that the fundamental mode is the $TM_{11\delta}$ mode, with the resonant frequency given by

$$f_{npm} = \frac{1}{2\pi a\sqrt{\mu\varepsilon}}\sqrt{X'_{np}{}^2 + \left(\frac{\pi a}{2h}\right)^2}\ \text{, where } X'_{11} = 1.841. \qquad (3.6)$$

The equations for the graph of resonant frequency and Q-factor of the $TM_{01\delta}$, $TE_{01\delta}$, and $HE_{11\delta}$ modes presented here are based on extensive numerical simulations and curve fittings.

$TE_{01\delta}$ Mode

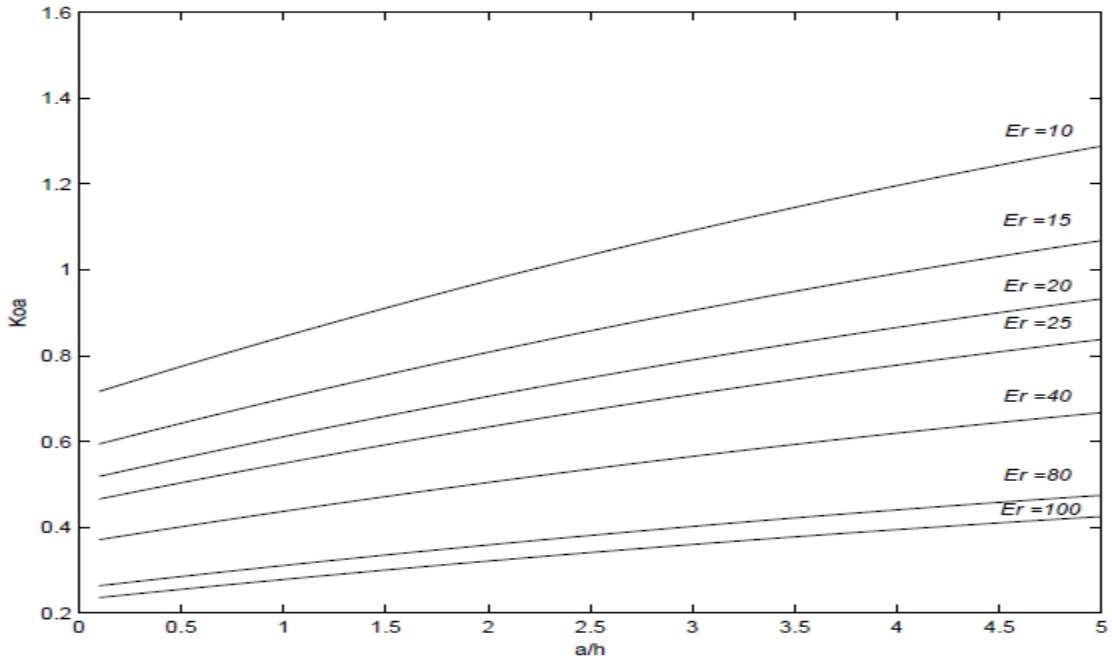

Figure 3. 6: k_o a of the $TE_{01\delta}$ mode of the cylindrical DRA

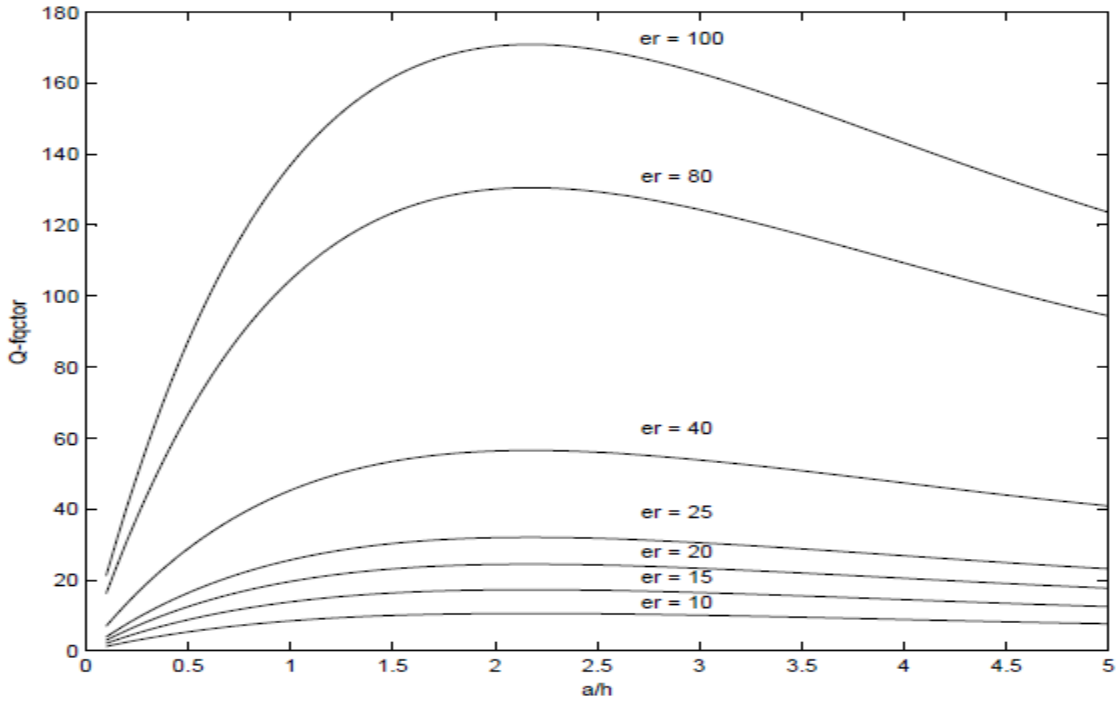

Figure 3. 7: Q-factor of the $TE_{01\delta}$ mode of the cylindrical DRA

$TM_{01\delta}$ Mode

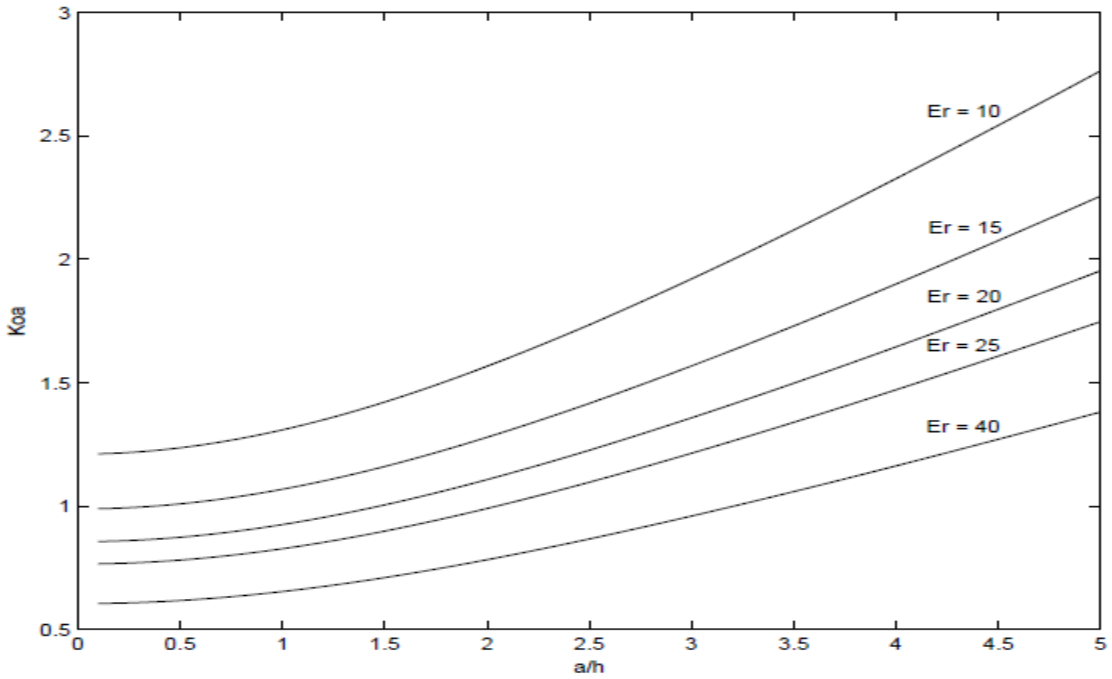

Figure 3. 8: $k_o a$ of the $TM_{01\delta}$ mode of the cylindrical DRA

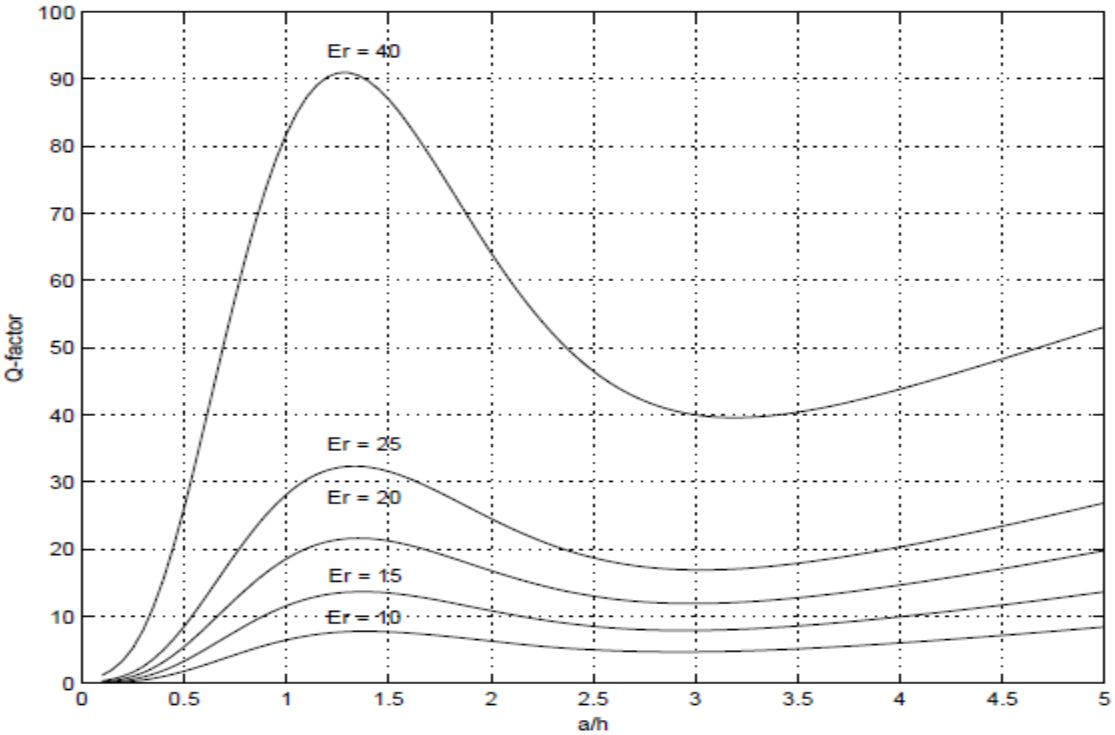

Figure 3. 9: Q-factor of the $TM_{01\delta}$ mode of the cylindrical DRA

$HE_{11\delta}$ Mode

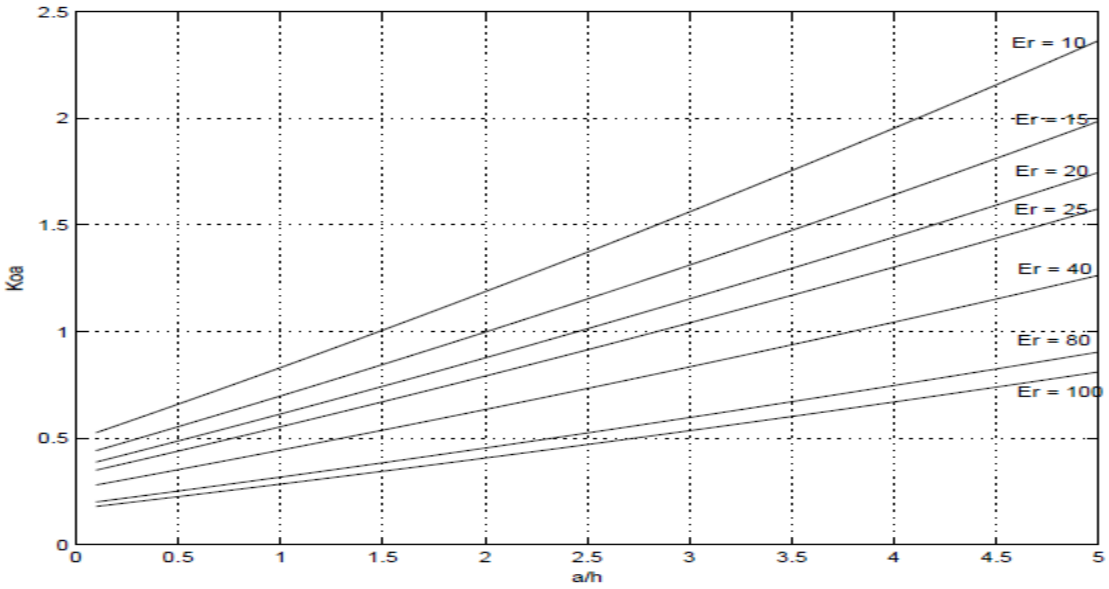

Figure 3. 10: k_o a of the $HE_{11\delta}$ mode of the cylindrical DRA

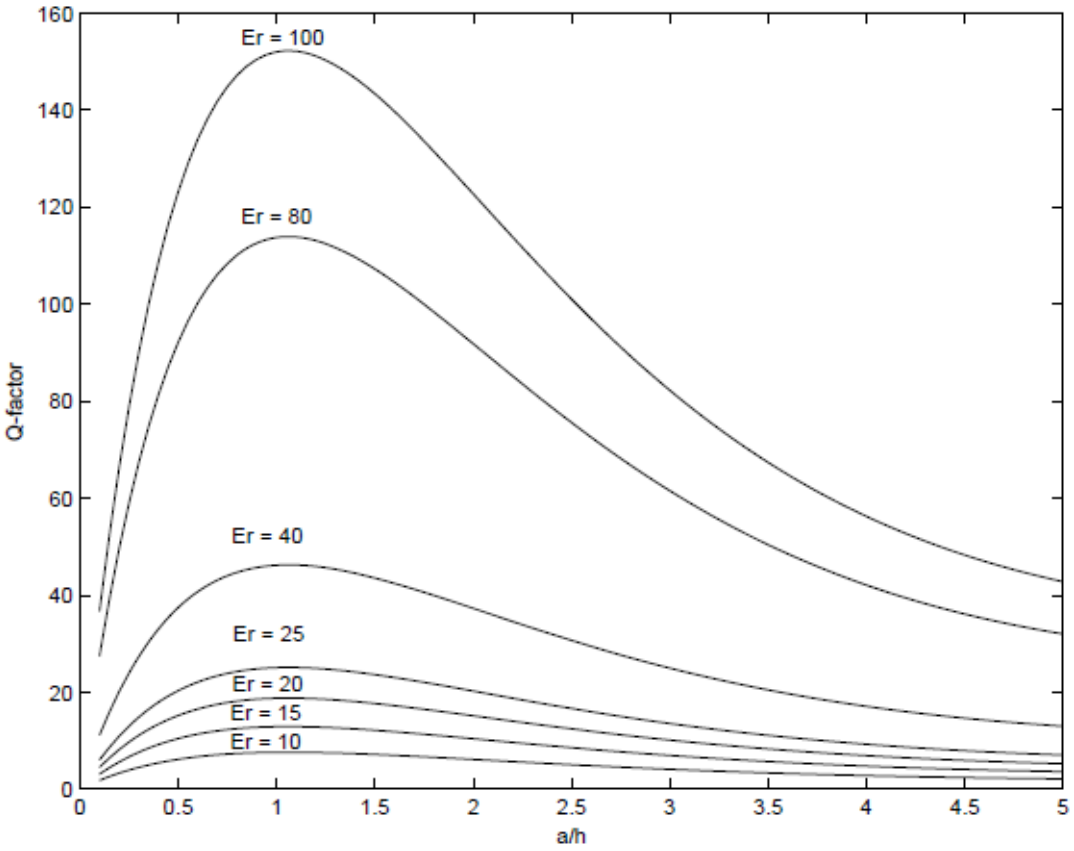

Figure 3. 11: Q-factor of the $HE_{11\delta}$ mode of the cylindrical DRA

3.2.2 Cylindrical DRA Design Example ($HE_{11\delta}$)

The same example is taken as for the hemispherical DRA, where a resonant frequency of 5.5 GHz and a minimum fractional impedance bandwidth of 8% is required.

Step 1. Determine the Q-factor.

This is the same as for the hemispherical DRA i.e. Q = 8.84

Step 2. Determine the dielectric constant.

Unlike the case for the hemispherical DRA, there is no unique value of dielectric constant for a given Q-factor. To determine the possible values of ε_r, the required Q-factor value is drawn on the Q-factor for the $HE_{11\delta}$ mode, as shown in figure. In general, the selection of ε_r depends on factors such as material availability and size requirements. For this example $\varepsilon_r = 10$ is taken.

Step 3. Determine $k_o a$ using

$$k_0 a = \frac{f_{GHz.}\, h_{cm}.(a/h)}{4.7713} \text{ with } f_{GHz.} = 5.5 \text{ GHz} \qquad (3.7)$$

Step 4. Determine the radius

by plotting Eq.(3.7) on the $k_o a$ vs. a/h graph for a set of values for h_{cm}. The intersection of these lines of constant 'h' with the curve for $\varepsilon_r = 10$ gives the value of a/h and thus the value for 'a' required to resonate at $f_{GHz} = 5.5$

3.3 The Rectangular DRA

The rectangular DRA is characterized by a height *h*, a width *w*, a depth *d*, and a dielectric constant ε_r as shown in fig 3.12

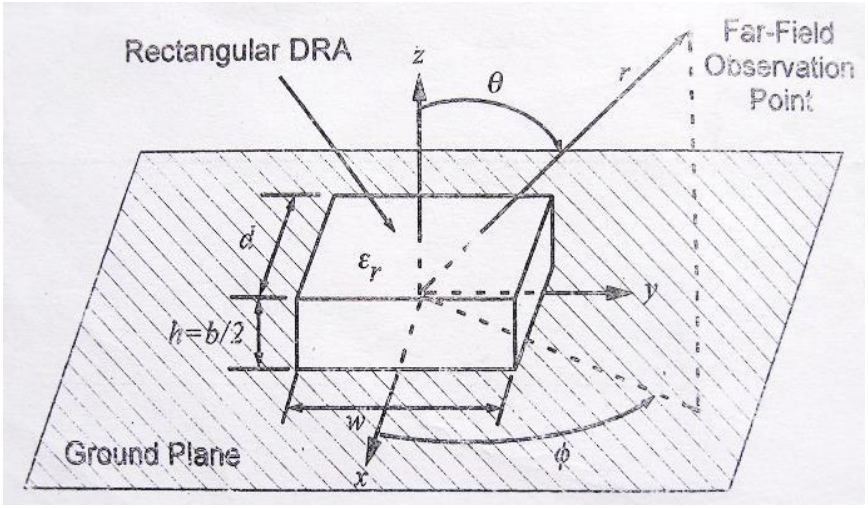

Figure 3. 12: The Rectangular DRA

The rectangular shape offers two degree of freedom (one more than the cylindrical and two more than the hemispherical DRA), making it the most versatile of the basic shapes. It has two aspect ratios *w/h* and *d/h*.

The modes in an isolated rectangular DRA can be divided into *TE* and *TM*, but with DRA placed on the ground plane, it is the *TE* modes which are typically excited. The rectangular DRA can support TE^x, TE^y, or TE^z modes which would radiate like the short magnetic dipoles in the *x*-, *y*-, and *z*- directions, respectively. The resonant frequency of each of these modes will be a function of the DRA dimensions.

The lowest order modes are $TE^x_{\delta 11}$, $TE^y_{1\delta 1}$, and $TE^z_{11\delta}$ for *w* > *d* > *b*. For the $TE^x_{\delta 11}$ mode, the resonant frequency f_0 is found by solving the following transcendental equation:

$$k_x \tan\left(\frac{k_x d}{2}\right) = \sqrt{(\varepsilon_r - 1){k_0}^2 - {k_x}^2} \qquad (3.8)$$

Where:

$$k_0 = \frac{2\pi}{\lambda_0}\ , k_y = \frac{\pi}{w}, k_z = \frac{\pi}{b} \text{ and } {k_x}^2 + {k_y}^2 + {k_z}^2 = \varepsilon_r {k_0}^2$$

3.3.1 Resonant Frequency and radiation Q-factor

Equation (3.8) is solved in Matlab for selected ratios of *w/b* as a function of *d/b*, and the results are plotted in fig , where the normalized frequency is defined as:

$$F = \frac{2\pi w f_0 \sqrt{\varepsilon_r}}{c} \tag{3.9}$$

It can be rearranged in easy form:

$$f_{GHz} = \frac{15F}{w_{cm}\pi\sqrt{\varepsilon_r}} \tag{3.10}$$

The radiation Q-factor of the rectangular DRA is determined using:

$$Q = \frac{2\omega W_e}{P_{rad}} \tag{3.11}$$

Where W_e and P_{rad} are the stored energy and the radiated power, repectively, and $\omega = 2\pi f_0$.

These quantities are given by:

$$W_e = \frac{\varepsilon_r \varepsilon_0 wbdA^2}{32}\left(1 + \frac{\sin(k_x d)}{k_x d}\right)\left(k_y^2 + k_z^2\right) \tag{3.12}$$

and

$$P_{rad} = 10 k_0^4 |\boldsymbol{p_m}|^2 \tag{3.13}$$

where

$\boldsymbol{p_m}$ is the magnetic dipole moment of the DRA:

$$\boldsymbol{p_m} = \frac{-j\omega 8\varepsilon_0(\varepsilon_r - 1)A}{k_x k_y k_z} sin(k_x d/2)\hat{\boldsymbol{x}} \tag{3.14}$$

and *A* is an arbitrary constant related to the maximum amplitude of the fields. Eq.(3.11) to (3.14) are used to generate the graphs in figures. These figures plot the normalized Q-factor (*Qe*) defined as:

$$Q_e = \frac{Q}{\varepsilon_r^{3/2}} \tag{3.15}$$

Since there is a second degree of freedom, the Q-factor curves cannot easily be plotted on a single graph, as was the case for the cylindrical DRA. Instead, a set of Q_e curves has to be plotted as a function of *d/b* for various values of *w/b*.

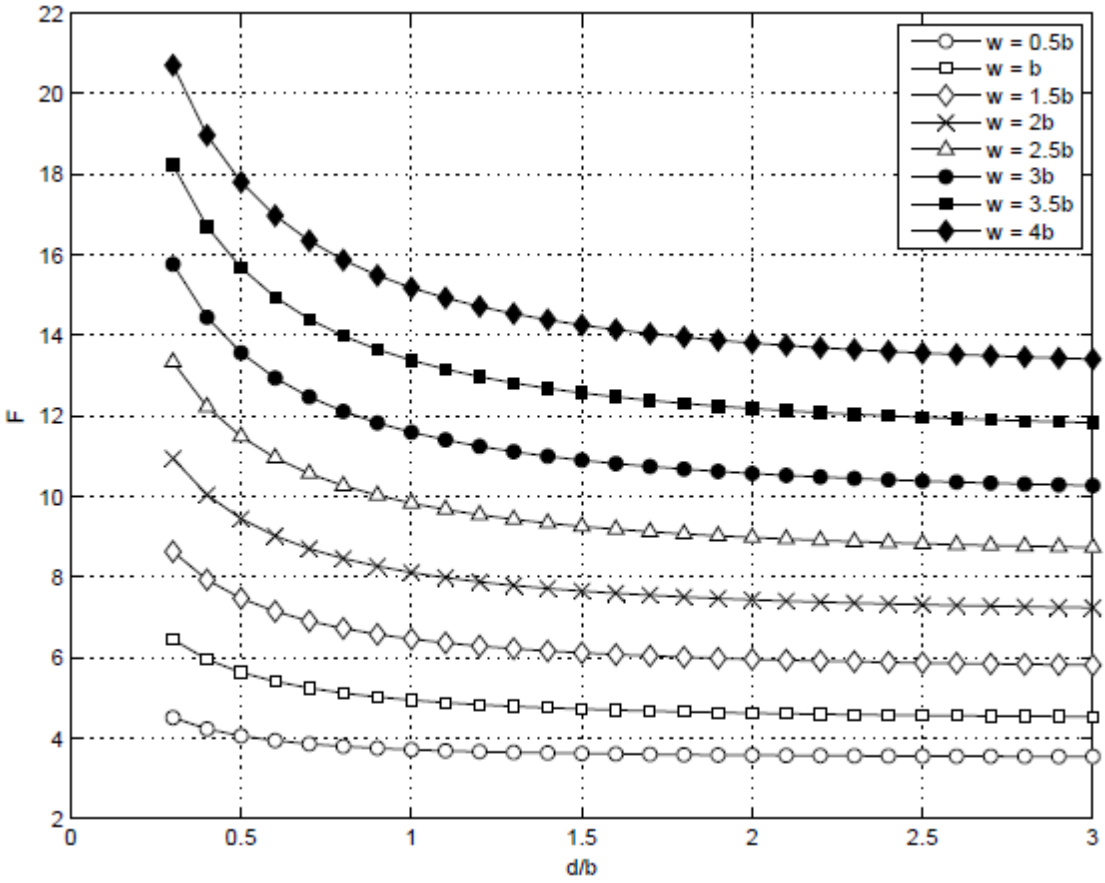

Figure 3. 13: Normalized resonant frequency of the rectangular DRA

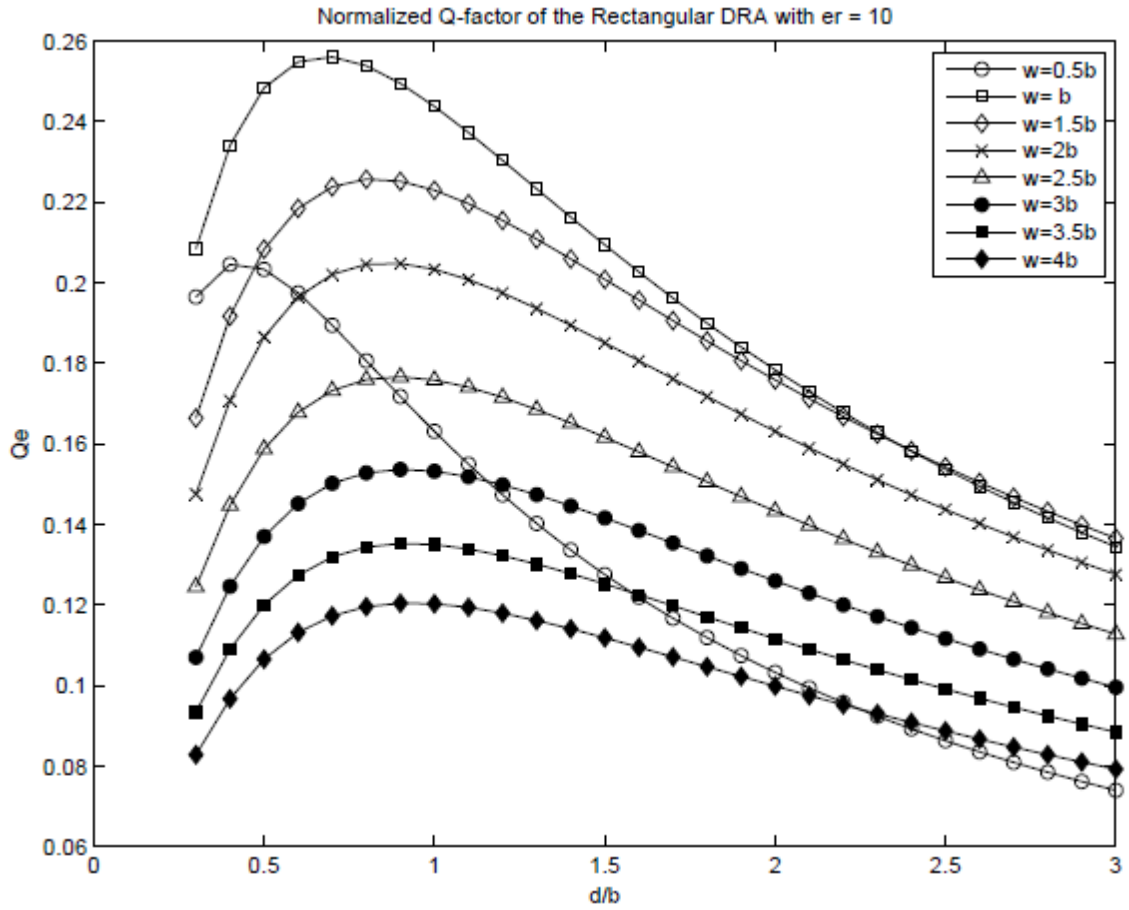

Figure 3. 14: Normalized Q-factor of the rectangular DRA (Ɛ_r=10)

3.3.2 Design procedure for the rectangular DRA

Step 1: Determine the Q-factor.

Step 2: Determine the dielectric constant.

Step 3: Determine F.

Step 4: Determine DRA dimensions (w, b, d).

Chapter 4

Coupling to DRA

In chapter 3, the design equations for predicting the resonant frequency and radiation Q-factor for the basic DRAs has been presented. While deriving these equations, it is assumed that the DRAs are in isolation or placed on an infinite perfect conducting plane and that the effect of feeding mechanisms is zero. But in fact, the selection of the feeding methods and its location w.r.t DRA, both play an important role in determining which modes are excited. They also slightly change the input impedance, resonant frequency, Q-factor and radiation characteristics of the isolated DRAs.

4.1 Review of Coupling Theory

For the proper working of DRA, energy needs be coupled into or out of it through one or more ports. The amount of energy coupled between the port and the DR antenna depends on the type of port used and the location of the port w.r.t. to the DRA. The frequency response of the impedance, amount of coupling, type of modes generated are all important to determine the performance of DRA. Without using numerical methods, these quantities are difficult to find. Nevertheless, it can be obtained approximately by knowing the field distribution of the isolated DRA, using Lorentz Reciprocity Theorem and coupling theory taken from resonator circuits.

Given two electric current sources, ***J1*** and ***J2*** in a volume *V* enclosed by a surface *S*, which give rise to electric fields ***E1*** and ***E2***, respectively, and two magnetic currents ***M1*** and ***M2*** giving rise to magnetic fields ***H1*** and ***H2***, then the Lorentz Reciprocity Theorem can be expressed as :

$$\oint_S (E_1 \times H_2 - E_2 \times H_1) \cdot dS = \int_V (E_2 \cdot J_1 - E_1 \cdot J_2 - H_2 \cdot M_1 - H_1 \cdot M_2) dV \tag{4.1}$$

which reduces to

$$\int_V (\boldsymbol{E}_1 \cdot \boldsymbol{J}_2 - \boldsymbol{H}_1 \cdot \boldsymbol{M}_2) dV = \int_V (\boldsymbol{E}_2 \cdot \boldsymbol{J}_1 - \boldsymbol{H}_2 \cdot \boldsymbol{M}_1) dV \tag{4.2}$$

According to the theorem the component of the electric field ***E1*** along source ***J2***, is the same as the component of the field ***E2***, along source ***J1***. The same is true for two magnetic sources and magnetic fields. When coupling to a DRA, there is typically only one source (either electric or magnetic) and the level of coupling, *k*, between the source and the fields within the DRA can be determined by applying (4.2) with the appropriate boundary conditions. For an electric source ***J1***,

$$k \propto \int_V (\boldsymbol{E}_2 \cdot \boldsymbol{J}_1) dV \tag{4.3}$$

and for a magnetic source ***M1***,

$$k \propto \int_V (\boldsymbol{H}_2 \cdot \boldsymbol{M}_1) dV \tag{4.4}$$

Equation (4.3) states that in order to achieve strong coupling using an electric current source (like a probe), then that source should be located in an area of strong electric fields within the DRA. On the other hand, to achieve strong coupling using a magnetic current source (like a loop) then from equation (4.4) the source should be located in an area of strong magnetic fields. It is thus necessary to have a good understanding of the field structures of the isolated

DRA, to determine where the feed should be placed to excite the appropriate mode in the DRA.

The Q-factor of the DRA is influenced by the loading effect of the coupling mechanism. An external Q-factor (*Qext*) is defined as:

$$Q_{ext} = \frac{Q}{k} \tag{4.5}$$

and the loaded Q-factor (Q_L) of the DRA is defined as:

$$Q_L = \left(\frac{1}{Q} + \frac{1}{Q_{ext}}\right)^{-1} = \frac{Q}{1+k} \tag{4.6}$$

Power transfer is maximum between the coupling port and the DRA when *k* is unity. This condition is called critical coupling. When $k < 1$, the DRA is said to be under coupled, while when $k > 1$, the DRA is over coupled. The following sections will review some of the more common coupling methods to DRAs.

4.2 Coupling Methods to DRA

The equations that have been presented in chapter 3 for the resonant frequency and Q-factors of the DRA do not take into consideration the method of coupling energy to the DRA. These coupling methods can have a significant impact on the resonant frequency and Q-factor, which the above equations fail to predict. This section gives a brief review of the various methods of coupling to DRAs.

4.2.1 Slot Aperture

Figure 4.1 illustrates a DRA fed by an aperture. Although a rectangular DRA is shown, aperture coupling is applicable to DRAs of any shape. It consists of a slot cut in a ground

plane and fed by a microstrip line beneath the ground plane. The aperture works like a magnetic current flowing parallel to the length of the slot, which excites the magnetic fields in the DRA. This coupling mechanism has the advantage of having the feed network located below the ground plane, thus avoiding spurious radiation.

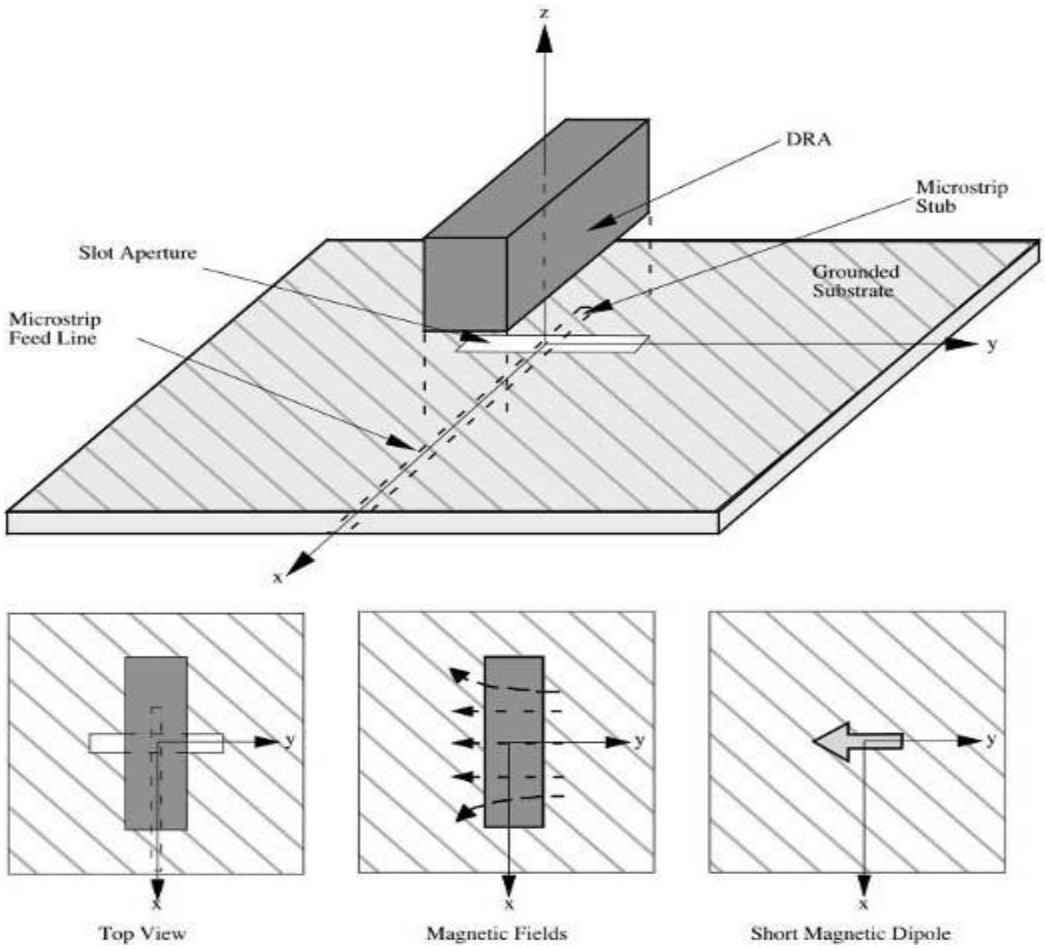

Figure 4. 1: Aperture fed DRA

4.2.2 Coaxial Probe

A coaxial probe is another common method for coupling to DRA as shown in Figure 4.2. The probe can either be located adjacent to the DRA or can be embedded within it. By adjusting

the probe height and its location w.r.t. DRA, the amount of coupling can be optimized. Also, depending on the location of the probe, various modes can be excited. Also, the excitation of various modes depends on the location of the probe.

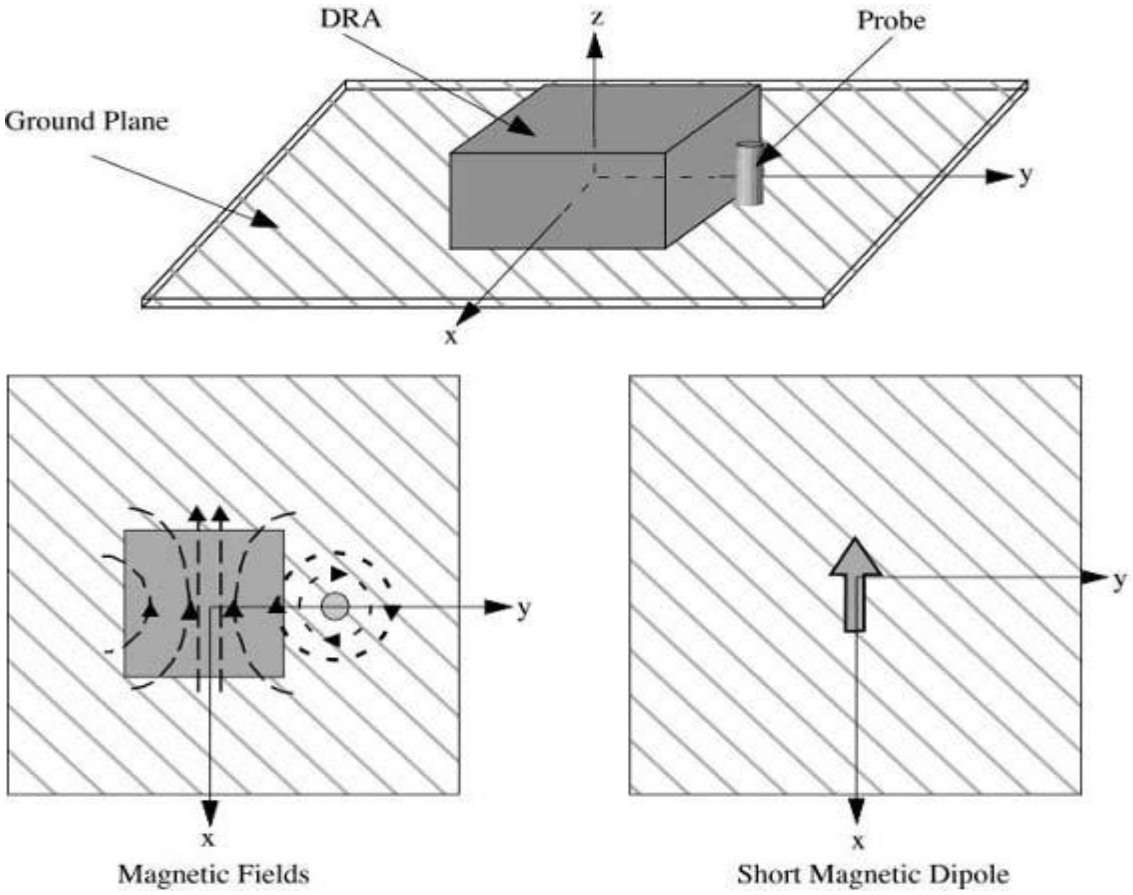

Figure 4. 2: Probe fed DRA

A probe placed adjacent to (or slightly inside) a rectangular DRA excites the $TE^{x}_{\delta 11}$ mode. Similarly, $HE_{11\delta}$ mode of a cylindrical DRA or the $TE_{01\delta}$ mode of the split cylinder can be excited with a probe located adjacent to (or slightly inside) the DRA. A probe located in the centre of a cylindrical DRA, excites the $TM_{01\delta}$ mode, as shown in. At lower frequencies aperture-coupling may not be practical due to the large size of the slot required. In that case Probes are useful.

4.2.3 Microstrip line

This method is as common as coaxial probe,shown in Figure 4.3. Microstrip coupling excites the magnetic fields in the DRA to realize the short horizontal magnetic dipole. The amount of coupling can be adjusted by the lateral position of the DRA with respect to the microstrip line and on the dielectric constant of the DRA. For lower dielectric constant values (necessary for DRAs requiring wide bandwidth), the level of coupling is generally quite small.

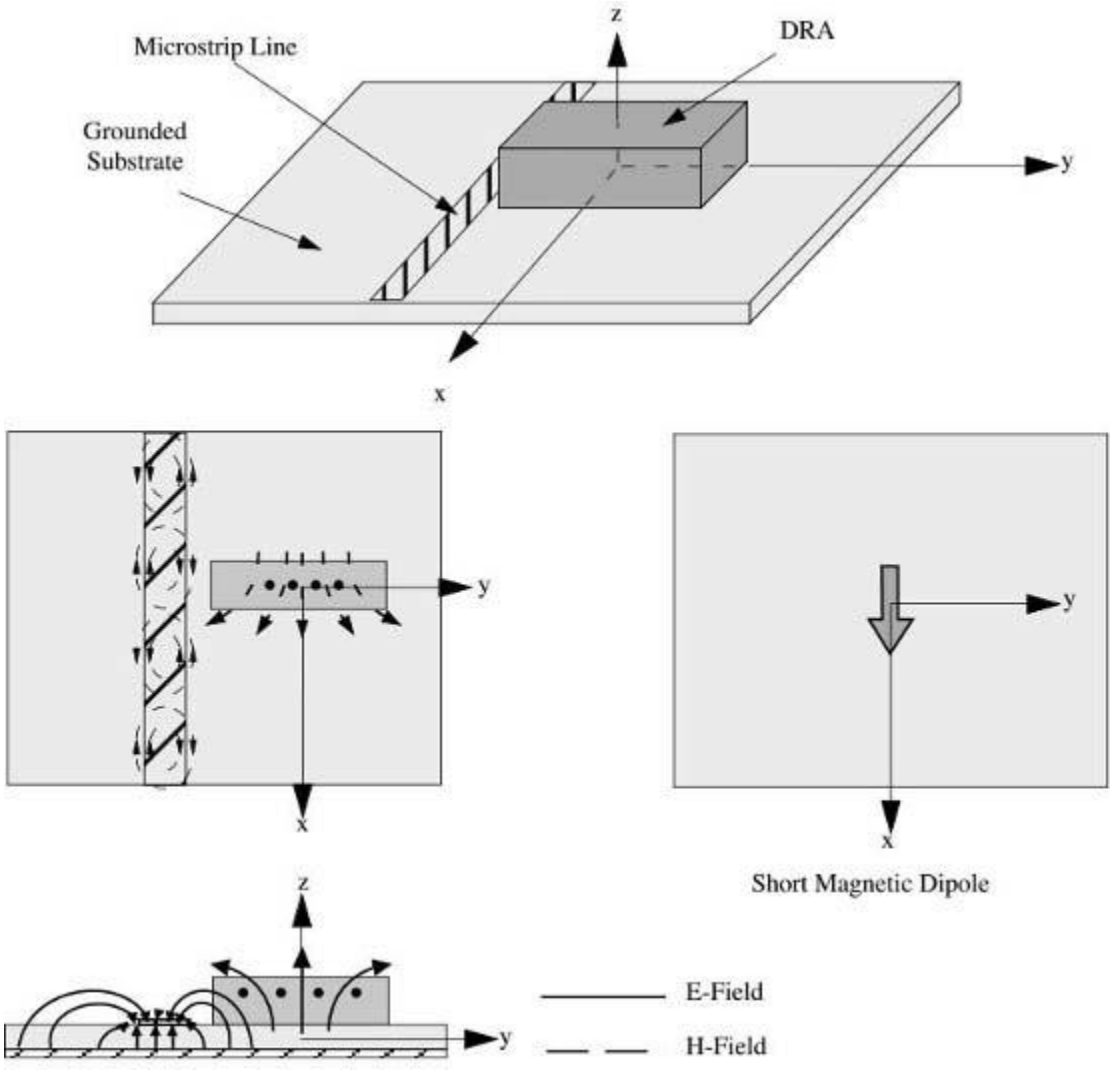

Figure 4. 3: Microstrip line fed DRA

4.2.4 Coplanar Feeds

Figure 4.4 illustrates a cylindrical DRA coupled to a co-planar loop. The amount of coupling can be adjusted by changing the location of the DRA over the loop. Its behaviour is similar to that of the coaxial probe, but the co-planar loop offers the advantage of being non-obtrusive. By moving the loop from the edge of the DRA to the centre, either the HE11δ mode or the TM011 mode of the cylindrical DRA can be coupled.

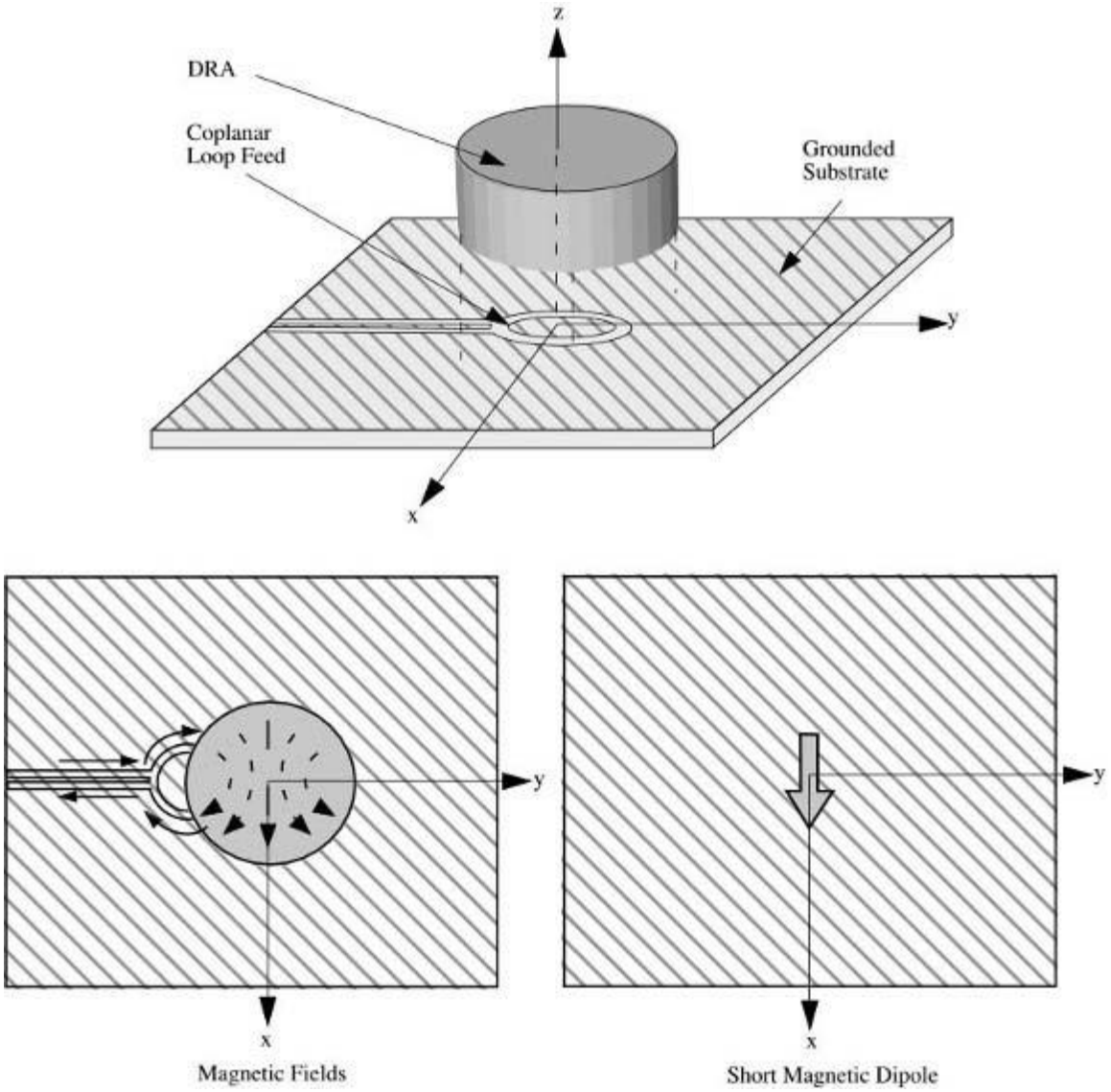

Figure 4. 4: Coplanar coupling

Chapter 5

Bandwidth Enhancement Techniques

The cylindrical and rectangular DRAs can have multiple design solutions for a given resonant frequency, permittivity and mode. However, the Q-factors for these solutions will be different. In this chapter the theoretical and practical lower limits of the Q-factor for cylindrical and rectangular DRAs is examined and then various methods to enhance the bandwidth is surveyed.

5.1 Bandwidth performance of basic DRAs

In chapter 3, a series of design curves for cylindrical and rectangular DRA is presented, in which Q-factor is shown as a function of ε_r and DRA dimensions. By looking at these curves, it can be observed that by choosing a low dielectric constant and the appropriate dimensions, a very low Q-factor can be obtained. This implies that it is theoretically possible to design an isolated cylindrical or rectangular DRA with a very broad bandwidth.

Table 5.1 summarizes the dimensions, resonant frequency, and Q-factor, based on the design equations and curves in chapter 3, for the case of isolated DRA. For a VSWR = 2, these DRASs could achieve bandwidths of up to nearly 40 %. Practically, wideband performance of these DRAs will be limited by the feeding methods.

Table 5. 1 Isolated DRAs with ε_r=10 designed for low Q-factor

Shape	*Mode*	*Dimension (mm)*	*f (GHz)*	*Q*	*Bandwidth*
Cylin.	$TE_{01\delta}$	a = 10, h = 2	6.15	5.4	13.5%
Cylin.	$TM_{01\delta}$	a = 10, h = 20	5.36	1.8	39.3%
Cylin.	$HE_{11\delta}$	a = 10, h = 2	11.28	2.1	33.7%
Rect.	$TE_{11\delta}$	w = 40, h = d = 5	6.71	3.4	20.8%

5.2 Bandwidth Enhancement for basic DRAs

The bandwidth of basic DRAs can be enhanced by an appropriate design of the feeding element or by introducing air gaps between the DRA and the ground plane.

5.2.1 Resonating Rectangular Slot Feed (Dual Resonance)

Generally, in the slot-fed DRA, the slot length is chosen to be below resonance to prevent unwanted radiation in the lower hemisphere (below the ground plane). By using a radiating slot, the impedance bandwidth can be significantly extended by setting up a dual resonance, but at the expense of backlobe radiations.

5.2.2 Ring-Aperture Feed

The aperture shapes used to feed DRAs in previous chapters were rectangular; however, other shapes can also be used. Fig.5.1 shows a cylindrical DRA fed by ring aperture.

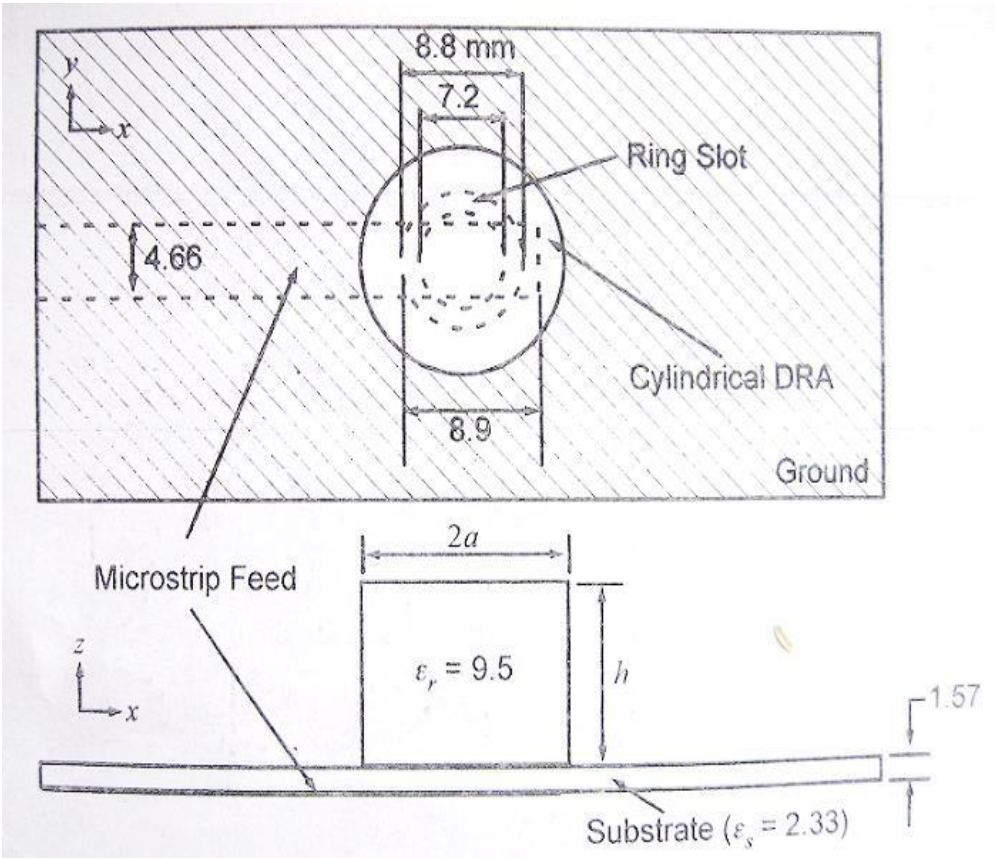

Figure 5. 1: Cylindrical DRA fed by a ring aperture

5.2.3 U-shaped-Aperture feed

A second example of a different shaped aperture used to feed a DRA is shown in fig 5.2. By using a U-shape slot, there are more parameters to tune the impedance response, compared to the simple rectangular slot.

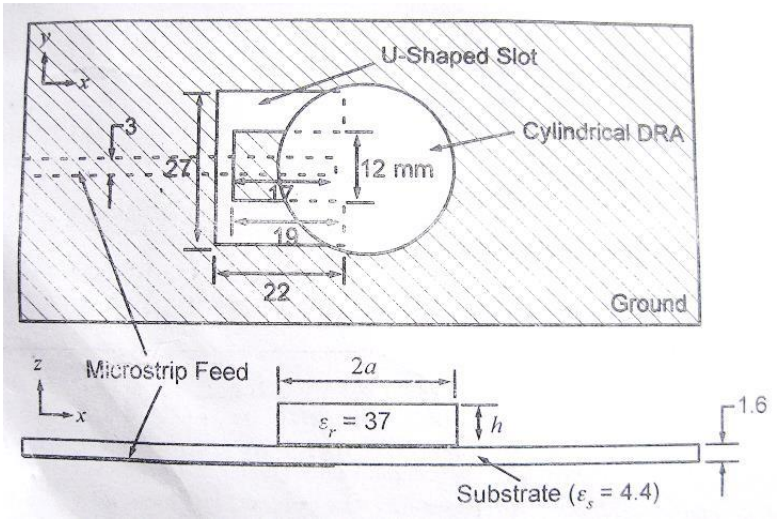

Figure 5. 2: Cylindrical DRA fed by U-shaped apeture

5.2.4 Microstrip fed DRAs

The bandwidth of microstrip fed rectangular and cylindrical DRAs can be enhanced by the addition of a simple microstrip-matching stub.fig 5.3

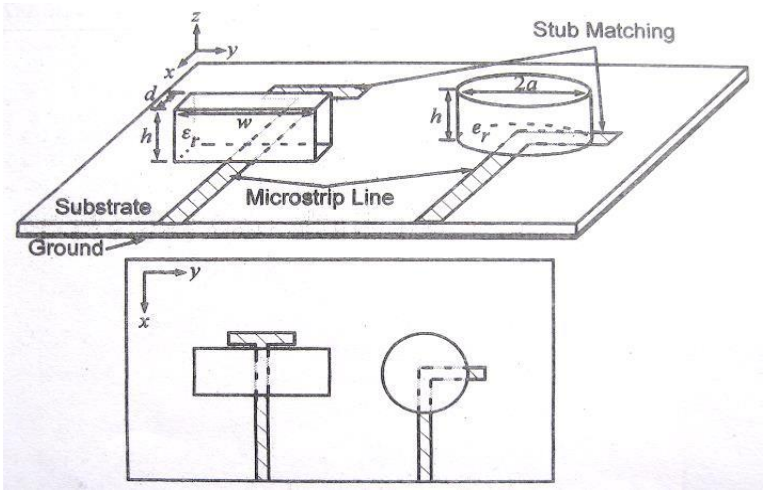

Figure 5. 3: Bandwidth enhancement with microstrip fed DRAs

5.2.5 Dual-Mode Recatangular DRAs

The impedance bandwidth of a DRA can be significantly increased by exciting two or more modes. However, the modes being excited should produce similar radiation patterns.

5.2.6 Ring DRAs

It consists of a cylindrical DRA where a central cylindrical section of radius 'b' is removed. Increasing the 'b/a' ratio results in an increase in the Q-factor; however, in order to maintain the same resonant frequency, the outer radius 'a' must be increased. For an approximate threefold increase in the outer radius, the Q-factor decreases by about 14 times.

5.3 Multiple DRAs

Here, the bandwidth enhancement by using two or more DRAs is explained. Each DRA is selected to resonate the same mode at somewhat different frequency, such that the combined response increases the overall bandwidth. A typical response of a two DRA configuration is shown in fig. If DRA1 has a normalized resonant frequency of f_l and bandwidth of Δf_l , while DRA2 has a normalized resonant frequency of f_u and bandwidth of Δf_u , then the combined response could have a bandwidth Δf that is larger than the sum of $\Delta f_l + \Delta f_u$, if f_l and f_u are properly chosen. If the assumption is made that the Q-factors of the resonator are approximately the same ($Q_1 \approx Q_2 = Q_0$) and if the return loss of the combined response should be equal to or better than 10 dB over the bandwidth *BW,* then the required values of resonant frequencies of the individual DRAs should be approximately equal to:

$$f_l \approx 1 - \frac{5}{6Q_0} \ , \ f_u \approx 1 + \frac{5}{6Q_0}$$

Assuming the bandwidths of the two DRAs are also similar ($\Delta f_l \approx \Delta f_l = \Delta f_0$), then the combined bandwidth is approximately $\Delta f \approx 3\Delta f_0$.

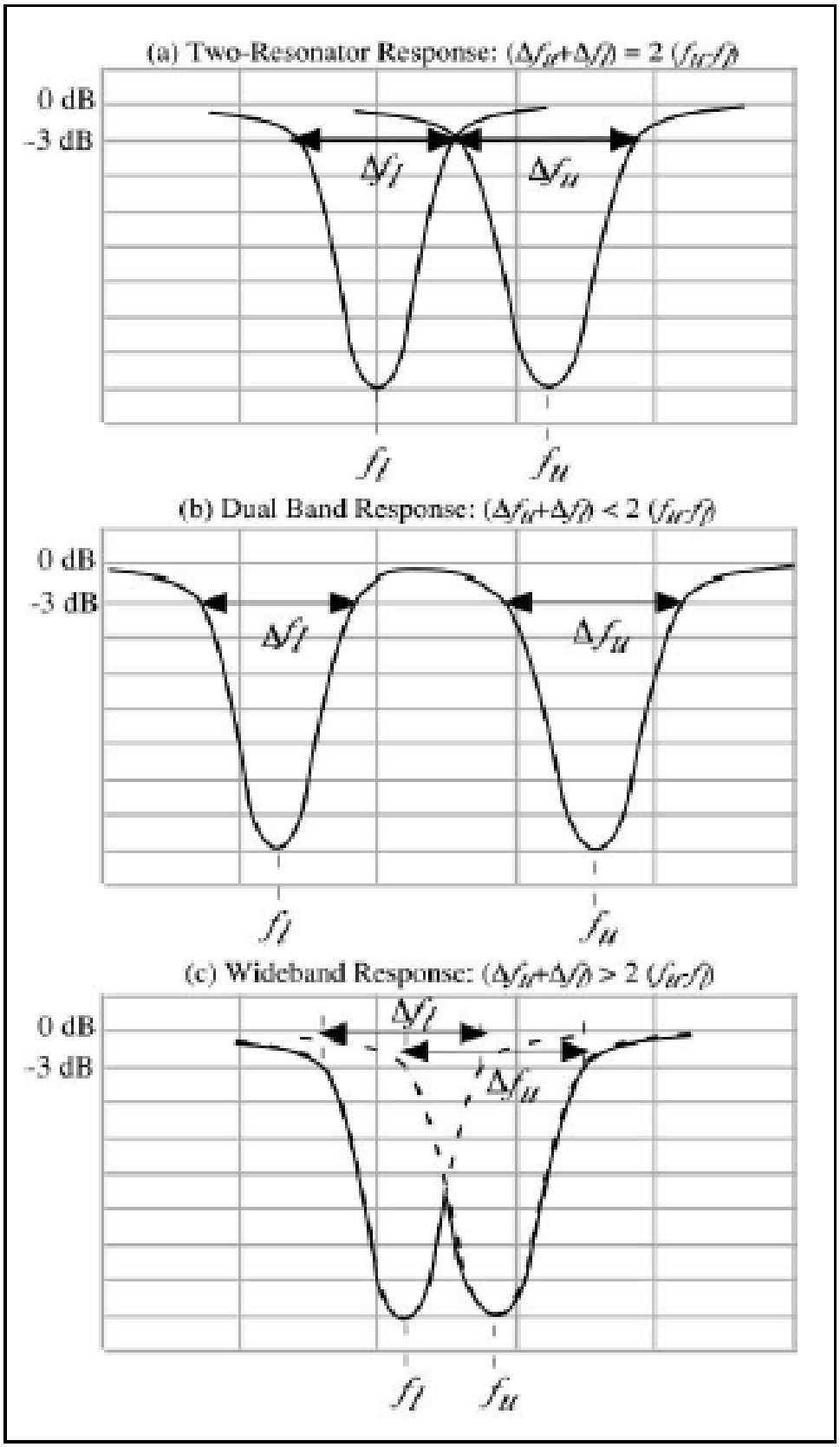

Figure 5. 4: Dual band and wideband response for a two-DRA configuration

5.3.1 Stacked DRA

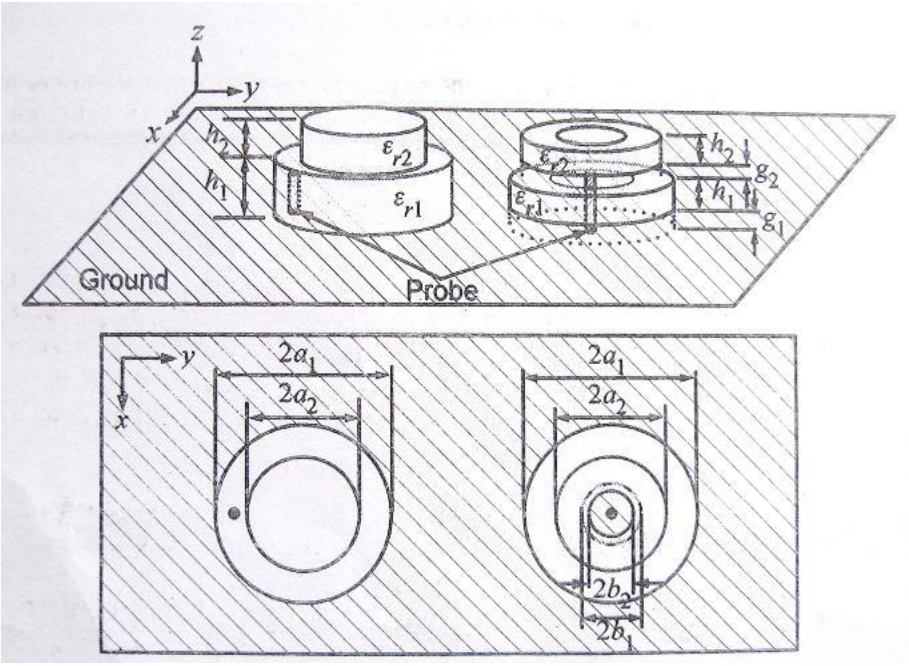

Figure 5. 5: Stacked DRAs

5.3.2 Coplanar DRAs

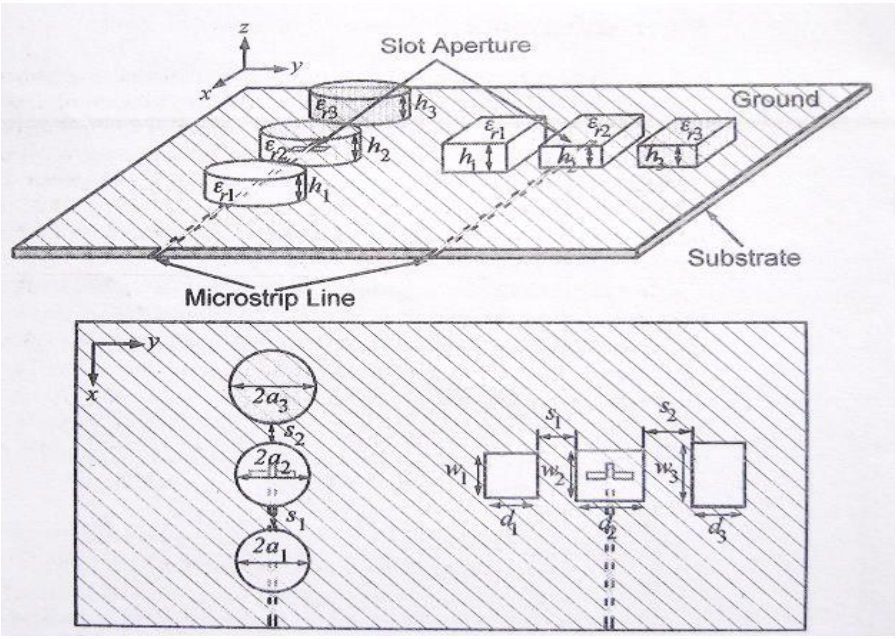

Figure 5. 6: Parasitic DRAs

5.3.3 Embedded DRAs

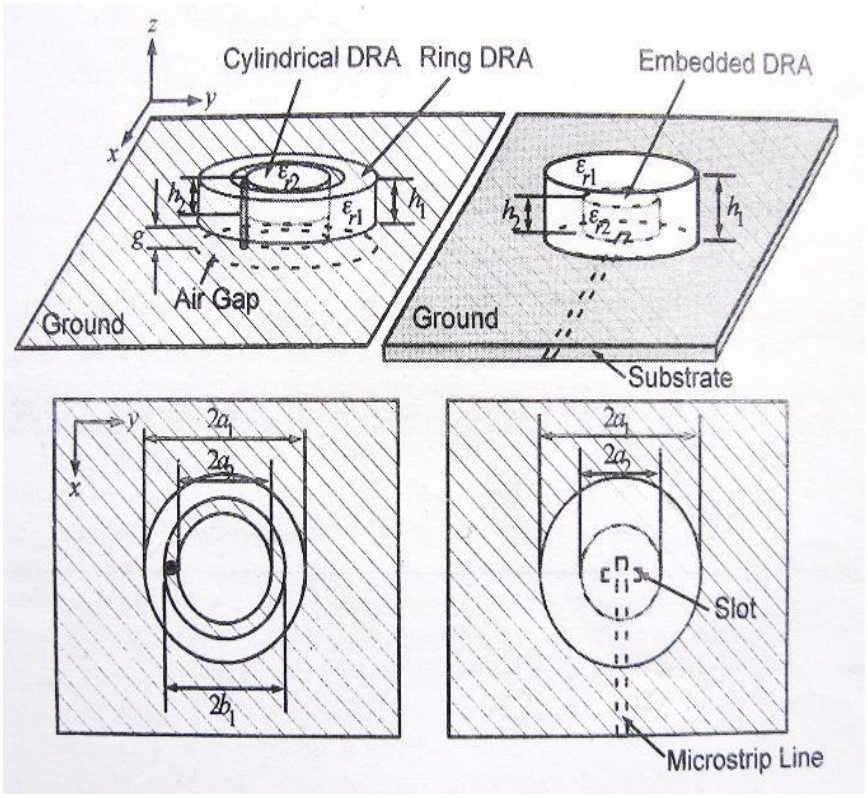

Figure 5. 7: Embedded cylindrical DRAs

5.4 Hybrid Antennas

In this section the bandwidth enhancement performance of hybrid antennas consisting of combination of DRA with either microstrip patch or a monopole antenna is shown.

5.4.1 DRA-Loaded Microstrip Patch Antenna

Microstrip patch antennas are commonly used because they are easy to fabricate. However, the bandwidth of a simple, single layer patch is typically quite narrow (1% to 2%). The bandwidth performance of patch antenna can be improved by loading it with a DRA, as shown in fig 5.8. Bandwidth of up to nearly 24% have been reported using this technique.

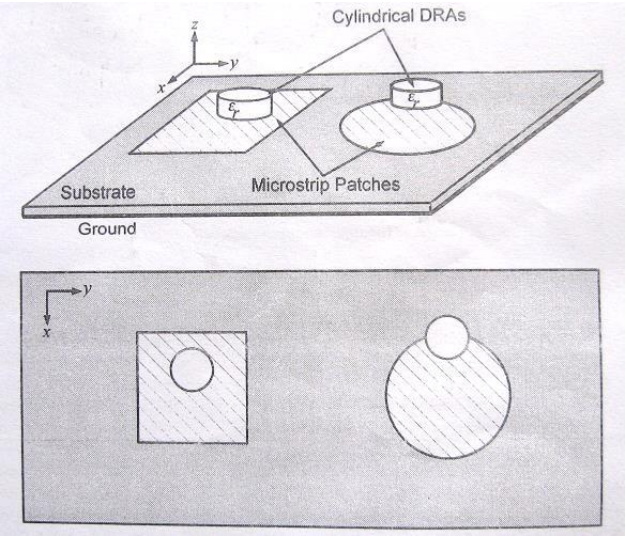

Figure 5. 8: DRA loaded patch antenna

5.4.2 DRA-Loaded Monopole Antenna

The bandwidth of a monopole antenna cab be significantly increased by the addition of a ring DRA, as shown in fig 5.9.The monopole and the ring DRA are both centred about the same axis, and the monopole simultaneously functions as quarter-wavelength radiator and as a feed for the DRA. The DRA is designed to operate in the $TM_{01\delta}$ mode, which has a circular symmetric modal field pattern similar to that of a short monopole antenna. This allows the centrally located monopole to efficiently excite the DRA. The monopole is designed to operate toward the lower end of the spectrum, while DRA operates toward the upper end. For wide band operation, the two resonant frequencies are chosen so that a min. return loss of 10 dB is obtained over the operating bandwidth. (The two frequencies can be separated further, if dual band operation is required instead of wideband).

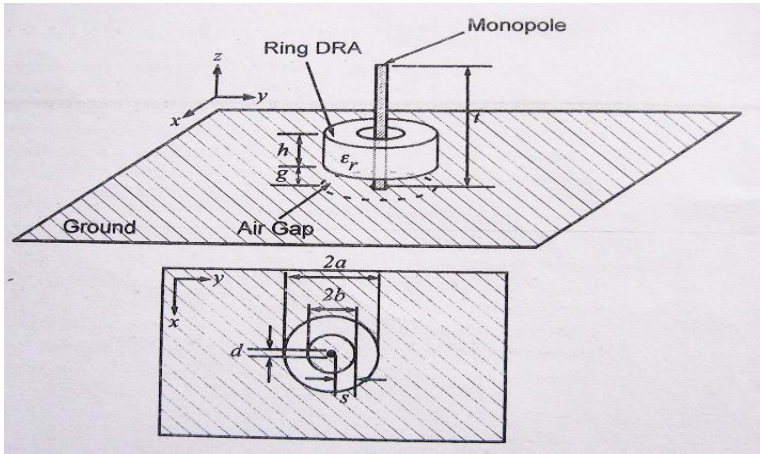

Figure 5. 9: DRA loaded monopole antenna

5.5 Modified DRAs

Bandwidth enhancement can be achieved by introducing some simple modification, such as carving a notch in the DRA, using a compound shape formed by simple discs or rect. DRAs, or altering the shape altogether.

5.5.1 Notched Rectangular DRA

A notch is introduced in the centre of the Rect. DRA as shown in fig. and by applying image theory, the notched DRA appears to a square ring as shown in fig 5.11 .By adjusting the dimensions (g, and l) of the notch, a dual band or wide band operation can be achieved

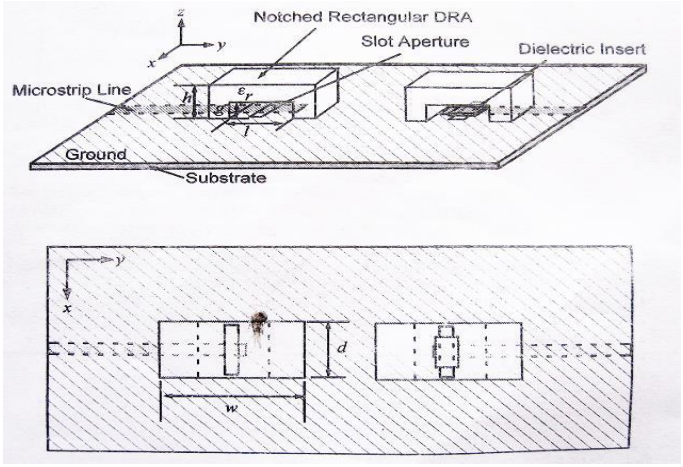

Figure 5. 10: Notched rectangular DRA

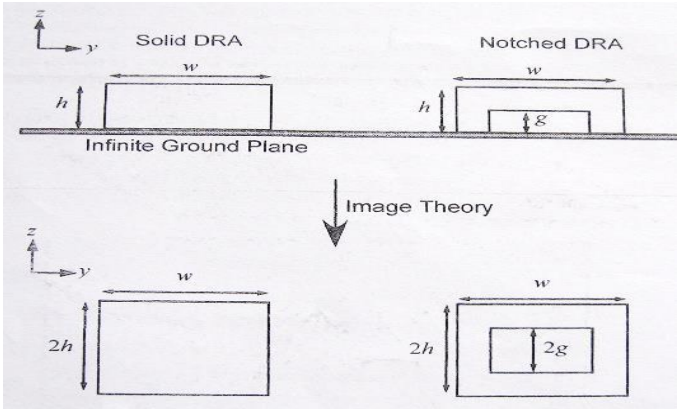

Figure 5. 11: Equivalent model of notched rectangular DRA using image theory

5.5.2 Inverted stepped pyramidal DRAs

Instead of using individual stacked DRAs, a single DRA can be fabricated into an inverted stepped pyramid as shown in fig 5.12. By adjusting the dimension of each of the steps, the location of the multiple resonances can be controlled to achieve a broadband response.

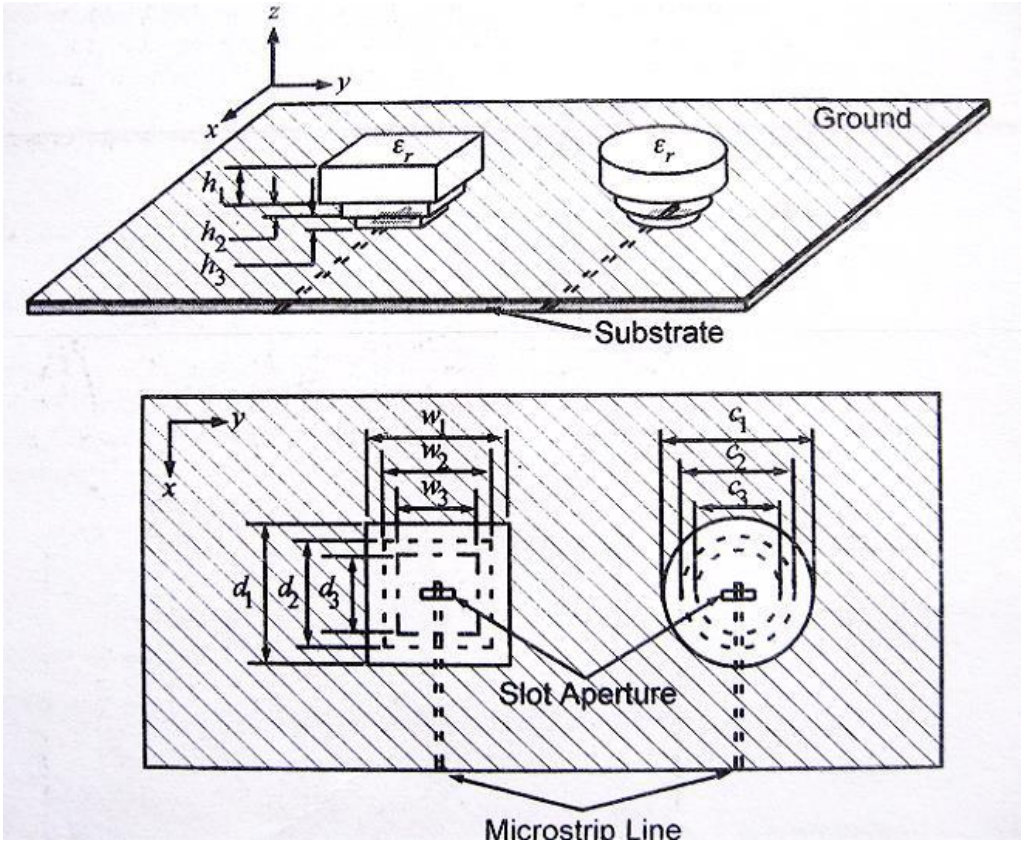

Figure 5. 12: Stepped DRAs

Chapter 6

Aperture Coupled Hemispherical DRA

In this chapter, the fundamental mode, TE_{111} mode of a hemispherical DRA excited by a microstrip line through a rectangular aperture is investigated. The effects of the slot length, slot width, and the stub length on the return loss and resonant frequency are studied and discussed.

6.1 Antenna geometry

The configuration of the DR antenna is shown in Figure 6.1, where the slot of length *L* and width *W* couples the energy from the microstrip line to the hemispherical DR of dielectric constant $\varepsilon_{rd} = 10$ and radius a = 8.2 mm which is got through the design equation for required resonant frequency of 5.2 GHz and 8% bandwidth . The slot is fed at the centre of the DRA.

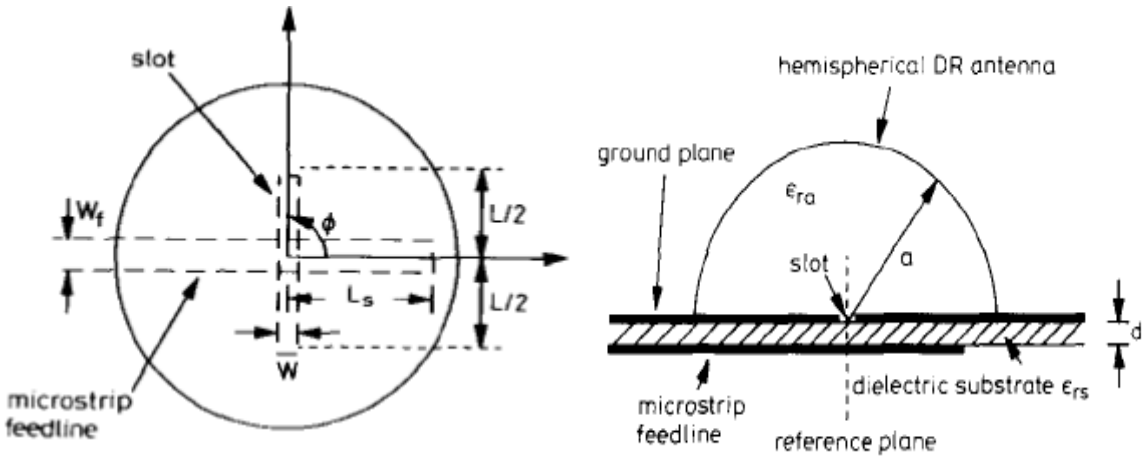

Figure 6. 1: Top and side view of hemispherical DRA.

The feed line is etched on the bottom side of FR4 substrate having dielectric constant of 4.4. The feed line is 2.85mm wide giving a characteristic impedance of 50 ohm at the frequency

of 5.2 GHz. The open stub at the end of the line is Ls = 7 mm, which is approximately $\lambda_g/4$ long.

6.2 Simulation Results

Figure 6.2 shows the plot between the slot length L and minimum return loss S11 with slot width W as parameter and stub length fixed at Ls = 7 mm. From the plot, the optimum slot length and width is found to be 8.5 mm and 1.5 mm repectively.

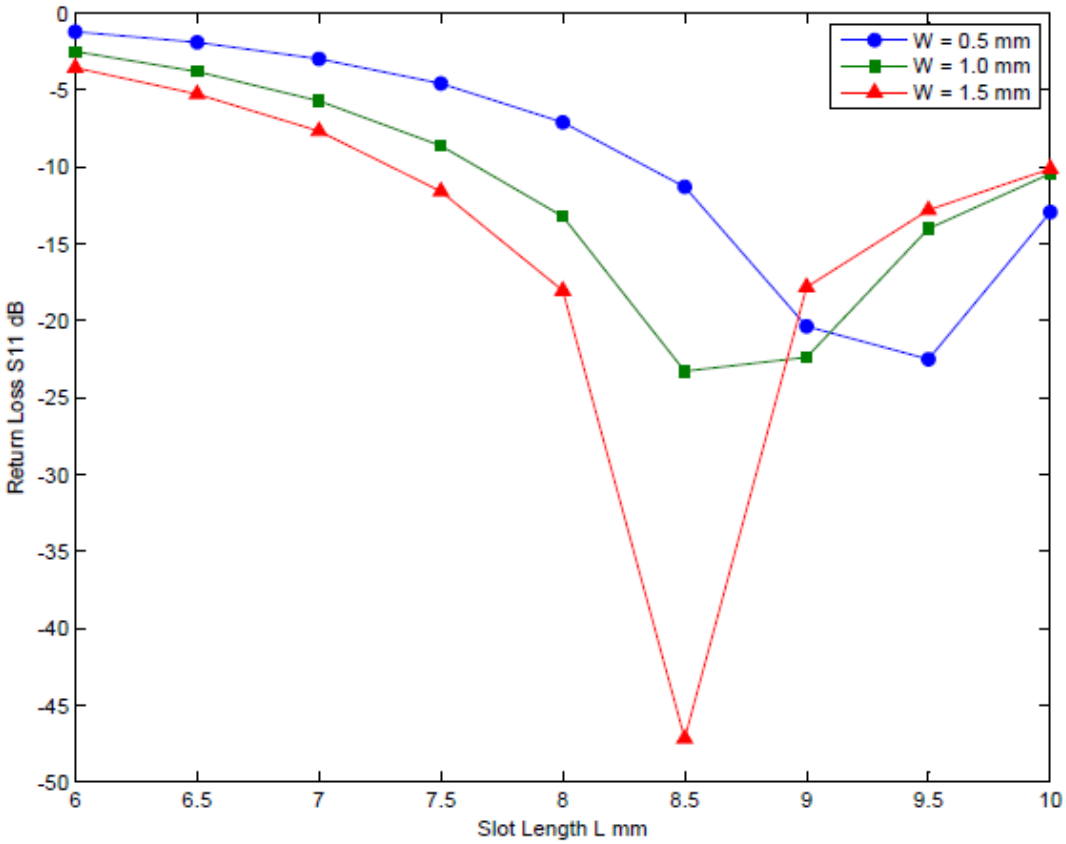

Figure 6. 2: Slot length v/s Return loss S11

Figure 6.3 shows the effect of changing slot length on resonant frequency with slot width as parameter. From the plot, it is clear that as the slot length and slot width increases, resonant frequency decreases.

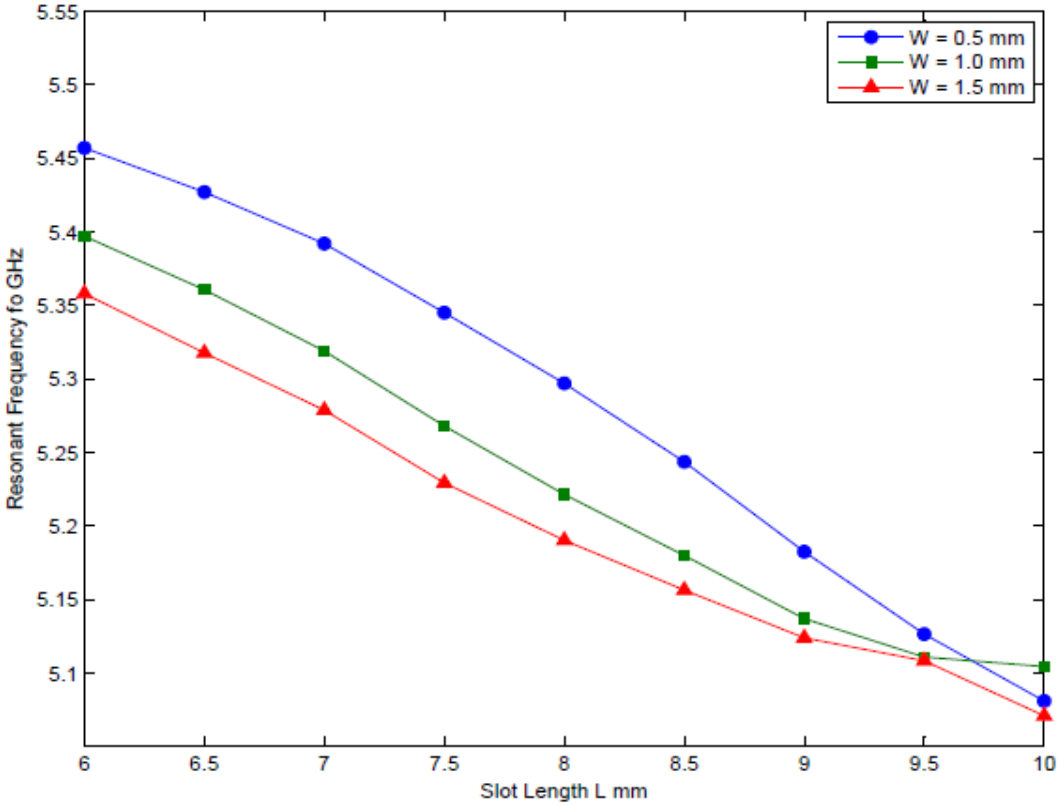

Figure 6. 3: Slot length v/s Resonant frequency

Table 7. 1 Dimension of Aperture Coupled Hemispherical DRA

Parameter name	Value	Description
a	8.2 mm	radius
d	1.6 mm	thickness of substrate
erd	10	permittivity of DRA
ers	4.4	permittivity of FR4
L	8.5 mm	length of slot
Ls	7 mm	stub length
W	1.5 mm	width of slot
Wf	2.85 mm	width of feed line

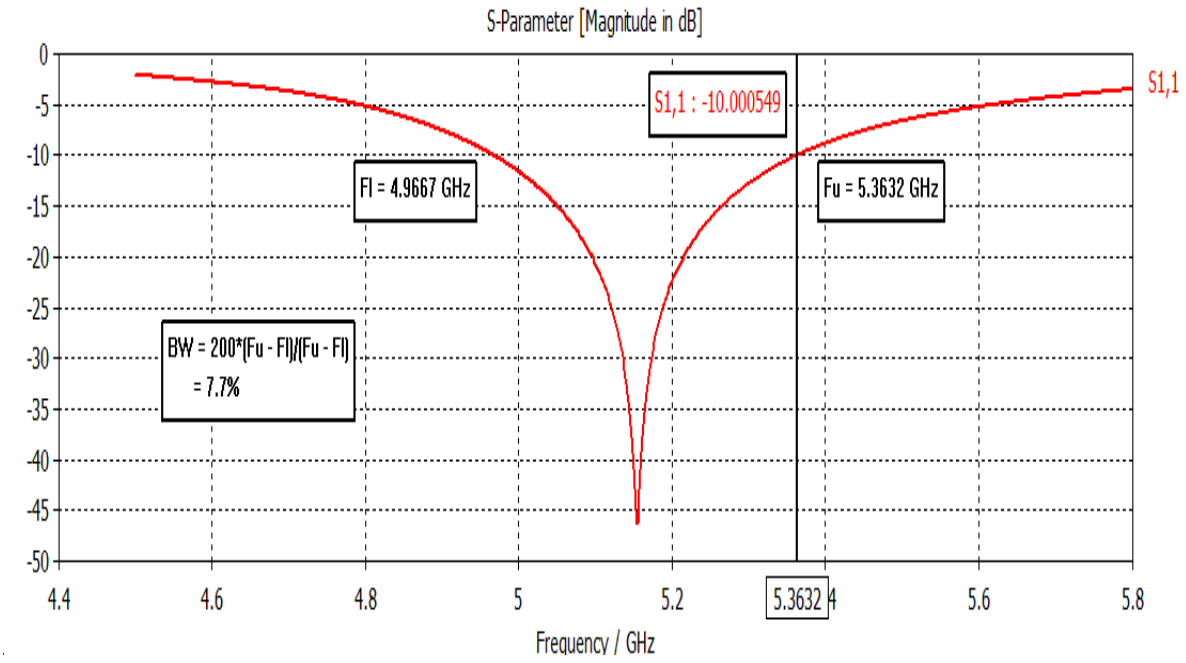

Figure 6. 4: Return Loss of Aperture Coupled Hemispherical DRA

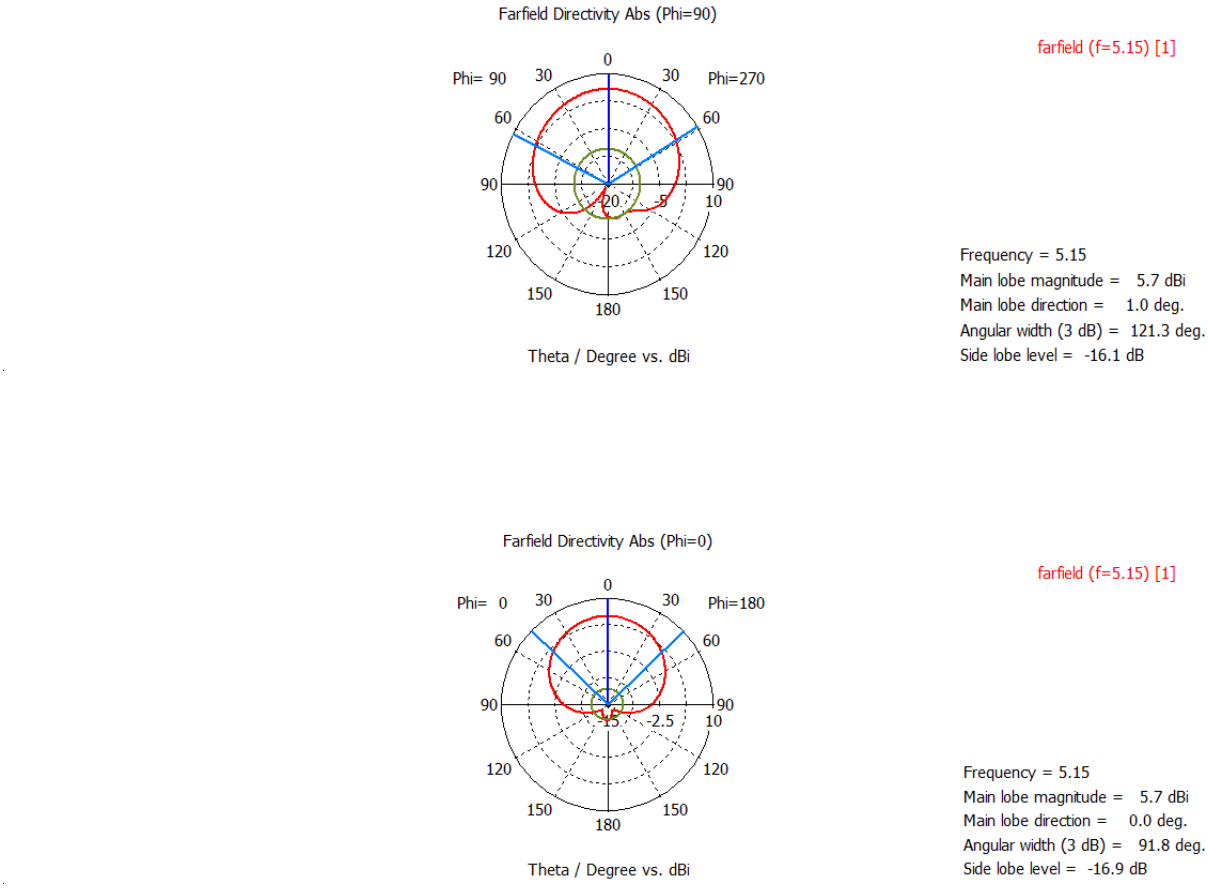

Figure 6. 5: E and H plane pattern of Aperture Coupled Hemispherical DRA

Chapter 7

Wide Band DRA (Hybrid and Modified DRAs)

7.1 Design 1: A wideband monopole antenna using dielectric resonator loading (Hybrid DRA).

As the future of wireless communication is driving toward broadband and dual band applications the use of a basic monopole antenna is becoming less suitable. To meet the emerging broadband services a monopole antenna must improve its bandwidth characteristic and provide the same level of simplicity while maintaining its omnidirectional pattern. This hybrid antenna design involves the use of a monopole antenna loaded with an annular ring dielectric resonator antenna (DRA) operating in the $TM_{01\delta}$ mode. In this arrangement both antennas produce a uniform horizontal coverage pattern.

7.1.1 Antenna Geometry

The Monopole-DRA antenna is shown in figure 7.1. It consists of a thin cylindrical monopole over a ground plane and an annular ring dielectric resonator antenna (DRA), both sharing the same axial reference. In this configuration, the monopole simultaneously performs the functions of a quarter wavelength radiator and as a feed for the DRA. The DRA is designed to operate in the $TM_{01\delta}$ mode, which has a circularly symmetric modal field pattern similar to that of a monopole antenna. This allows the centrally located monopole to efficiently excite the DRA. This arrangement could be described as two cascaded resonating circuits, which resonate at two different frequencies. The monopole is designed to operate at the lower end of the spectrum while the DRA operates at the upper end.

There are a number of parameters that influence the general behaviour of this configuration. These include the length of the monopole, the size and permittivity of the DRA, and the size of the ground plane. Dimension of DRA is given in table 7.1.

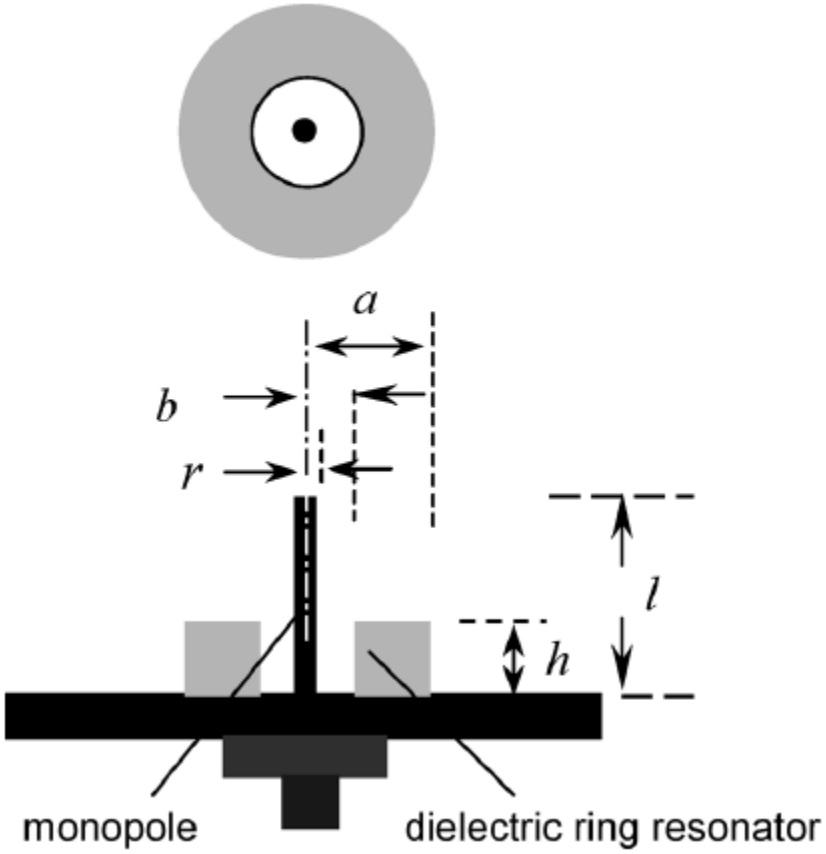

Figure 7. 1: Top and cross-sectional views of Monopole-DRA

The monopole length is chosen to resonate at the lower end of the bandwidth and the DRA at about twice that frequency. To set the resonant frequency of the DRA, two main factors are considered. First the height of the DRA is chosen so as not to completely cover the monopole and significantly affect its radiation into free space. At the same time the DRA should be high enough, in relation to its outer radius, to act as a resonator. To do so the height of the DRA was selected to be close to half the length of the monopole. Then the outer diameter of the dielectric ring is calculated using design equations in chapter 3 to achieve the proper resonant frequency. As a final step, the inner diameter of the DRA is varied to achieve a good matching of the quarter wave monopole antenna to a 50 ohm coaxial feed line.

Table 7. 1 Dimension of the DRA-loaded Monopole antenna

Parameter name	Value	Description
erd	15	permittivity of DRA
ers	4.4	permittivity of FR4
l	13.4 mm	length of monopole antenna
R	25 mm	radius of circular substrate
a	4.5 mm	outer radius of cylindrical DRA
b	.9 mm	inner radius of cyl.DRA
d	1.6 mm	thikness of substrate
h	6 mm	height of DRA
rc	2.24 mm	radius of coaxial cable insulator
r	.65 mm	radius of inner conductor of coax

7.1.2 Simulation Results

Figure 7.2 and 7.3 show the simulated return loss (S11) of the unloaded Monopole and the Monopole antenna loaded with DRA respectively. Both works in the C-band (4-8 GHz). The frequency range of the unloaded monopole antenna is from 4.67 GHz to 5.6 GHz equivalent to impedance bandwidth of 18.4%. The Monopole-DRA is matched within the frequency range of 4.89 GHz to 9 GHz equivalent to impedance bandwidth of 59.2%. Figure 7.4 shows the 3D radiation pattern of Monopole-DRA that gives the directivity of 3.36 dBi at the frequency of 6.5 GHz. While the directivity of unloaded monopole is only 2.1 dBi.

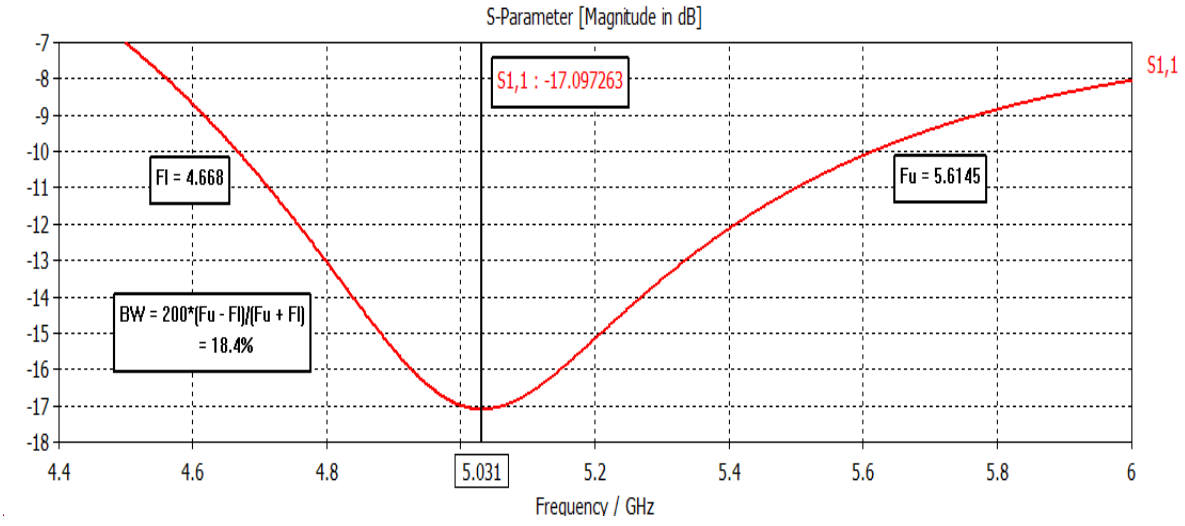

Figure 7. 2: Return loss of Unloaded Monopole antenna

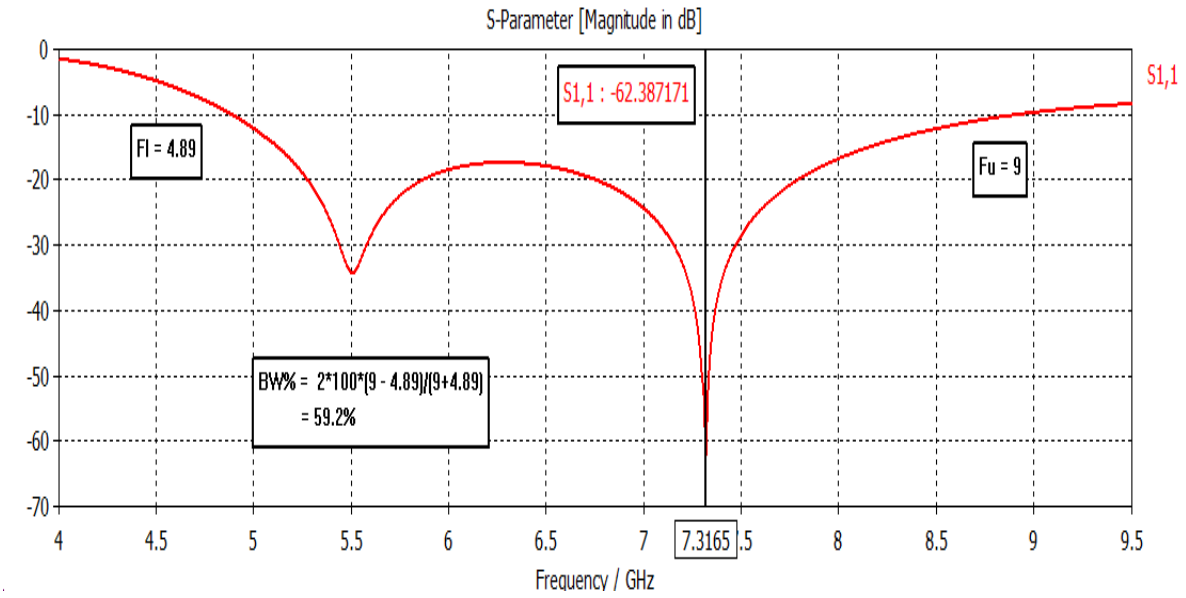

Figure 7. 3: Return loss of DRA-loaded Monopole antenna

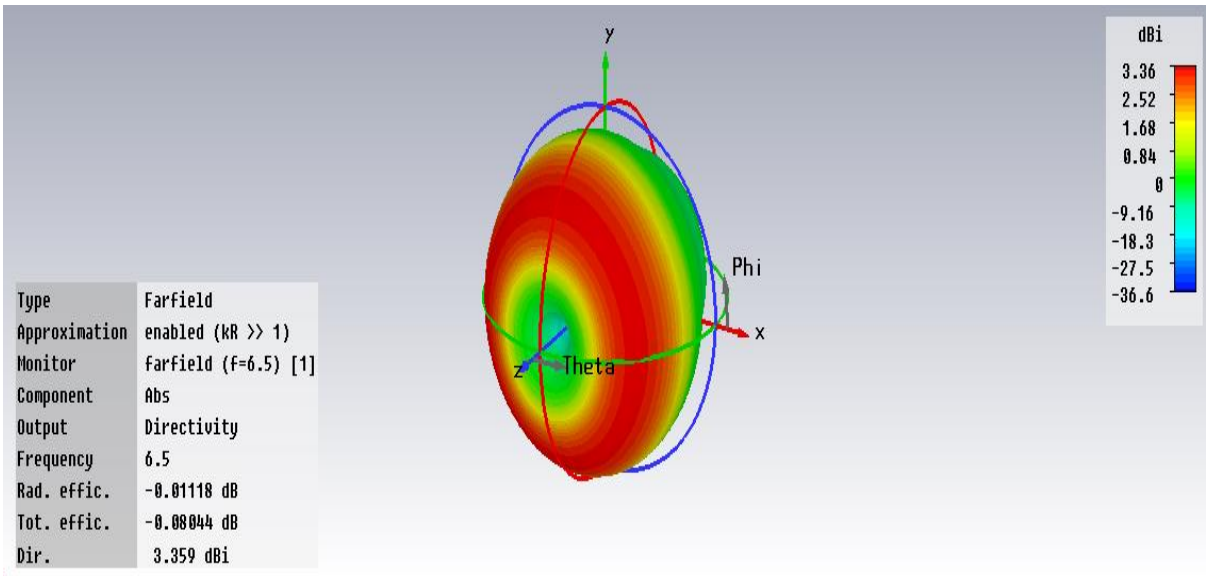

Figure 7. 4: 3D radiation pattern of DRA-loaded Monopole antenna

7.2 Design 2: Broadband Aperture Coupled Flipped Staired Pyramid and Conical DRA. (Modified DRA)

In this section, broadband DRAs using narrow slot aperture coupled to a microstrip line feed are designed. Two different shapes of dielectric resonators tapered in a stair-like structure have been designed for wideband applications. The resonators are located at the centre of the rectangular slot and are excited by centre feed microstrip line. Two flipped step stair shaped dielectric resonators with square and cylindrical cross sections are designed to give an impedance bandwidth of 49.7% and 35.9%, respectively. They have broadside radiation patterns across the matching band with an average gain higher than 6dbi. The simulation results are obtained by using CST Microwave Studio.

7.2.1 Antenna Geometry

Figure 7.5 show the geometry of the DRAs with square and cylindrical shapes, respectively. Both structures are constructed on 3-steps flipped stair geometry. The dielectric constants of both DRAs are equal to 12. Detailed dimensions of square shape and cylindrical shape DRAs are shown in Table 7.2 and 7.3 respectively.

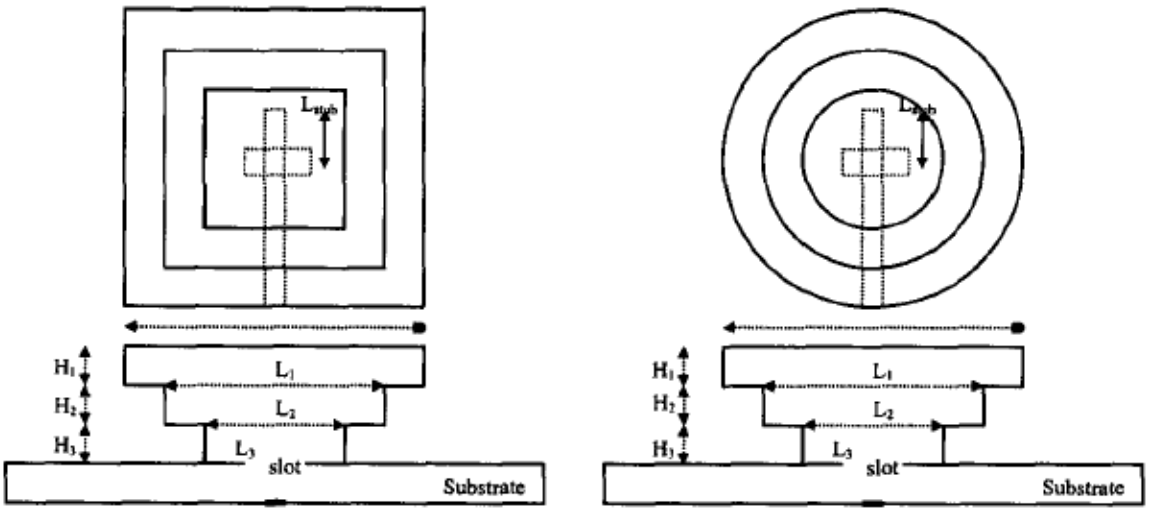

Figure 7. 5: Geometry of the Flipped Staired DRA

Table 7. 2 Dimension of Flipped Staired Pyramid DRA

Parameter name	Value	Description
H1	1.8 mm	height of top square
H2	1.3 mm	height of middle square
H3	1.3 mm	height of bottom square
L1	14 mm	length of top square
L2	8 mm	length of middle square
L3	6 mm	length of bottom square
Ls	5.6 mm	Length of slot
S	4 mm	stub extension
Wf	1.76 mm	width of feed line
Ws	.5 mm	width of slot
erd	12	dielectric constant of DRA
ers	4.4	dielectric constant of FR4 substrate
h	1.6 mm	substrate thickness

Table 7. 3 Dimension of Flipped Staired Conical DRA

Parameter name	Value	Description
H1	2.2 mm	height of top cylinder
H2	1.3 mm	height of middle cylinder
H3	1.3 mm	height of bottom cylinder
L1	11 mm	diameter of top cylinder
L2	8 mm	diameter of middle cylinder
L3	5.5 mm	diameter of bottom cylinder
Ls	5.5 mm	length of slot
S	4.6 mm	stub length
Wf	1.76 mm	width of feed line
Ws	.5 mm	width of slot
erd	12	dielectric constant of DRA
ers	4.4	dielectric constant of FR4
h	1.6 mm	substrate thickness

7.2.2 Simulation Results

Figure 7.6 and 7.7 show the simulated return loss (S11) of the square shape and cylindrical shape DRAs respectively. The DRAs are designed to operate in the X-band. The frequency range of the square shape DRA is from 7.82 GHz to 13 GHz, equivalent to an impedance bandwidth of 49.7% (S11 < -10 dB). The cylindrical shape DRA is matched within the frequency range of 8.8 GHz to 12.65 GHz with an impedance bandwidth of 35.9%.

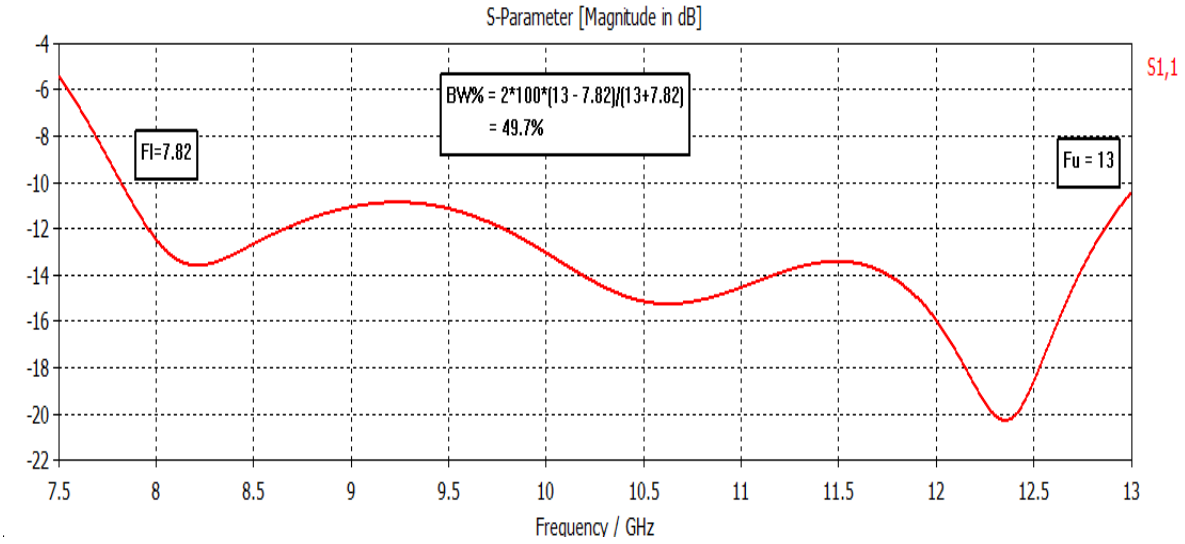

Figure 7. 6: Return loss (S11) of the square shape DRA

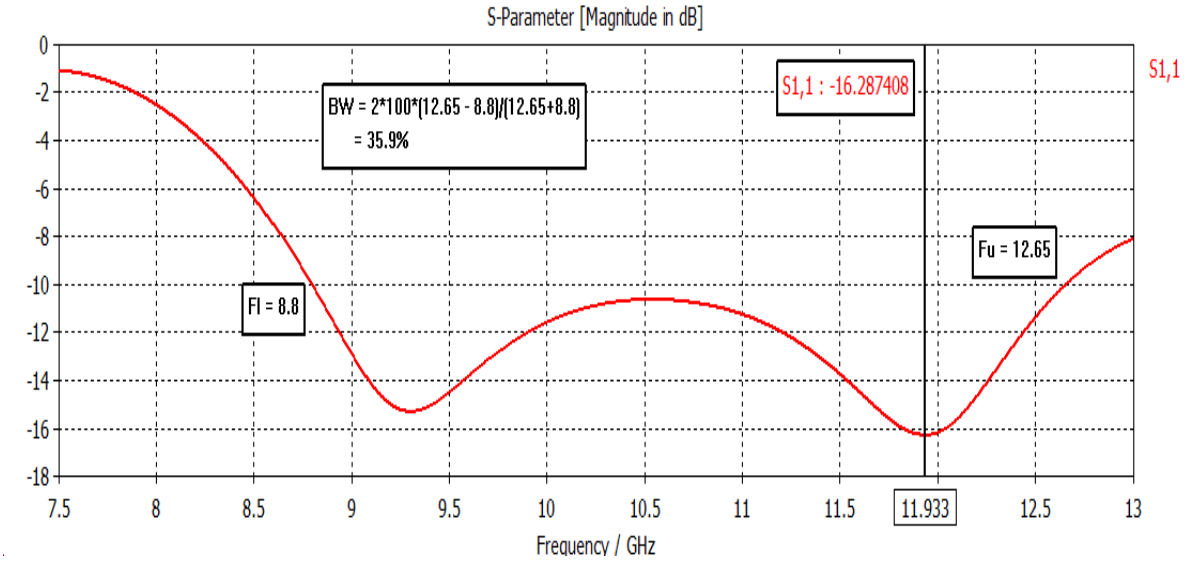

Figure 7. 7: Return loss (S11) of the Cylindrical shape

Figure 7.8 shows the E-plane and H-plane radiation pattern of the square shape DRA, respectively. The aperture coupled DRA radiates in the broadside direction and is symmetrical along the H-plane (xz-plane). Figure 7.9 shows the E-plane and H-plane radiation pattern of the circularly shaped DRA, respectively. It also has similar radiation properties as the square shape DRA. Figure 7.10 shows the maximum gain

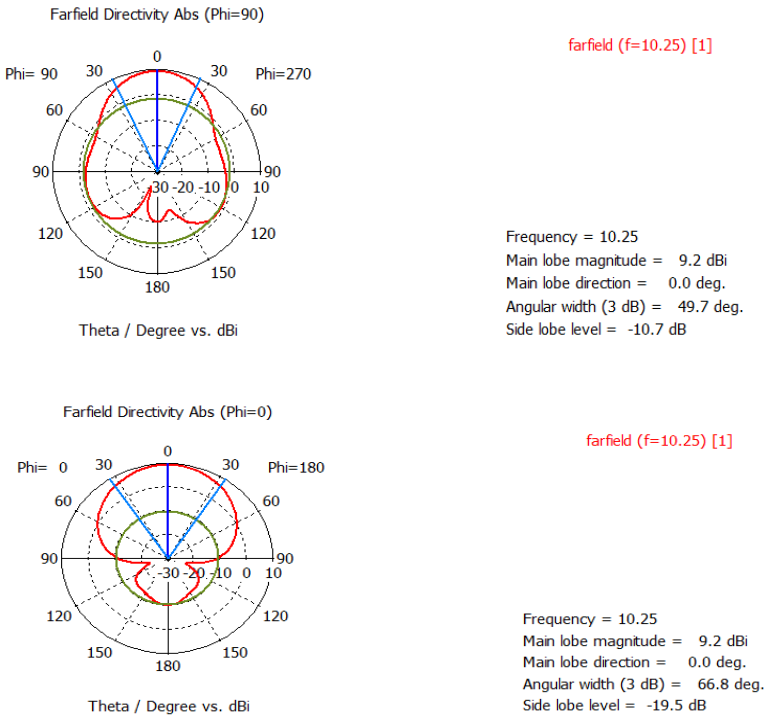

Figure 7. 8: E and H plane radiation pattern of Square shape DRA

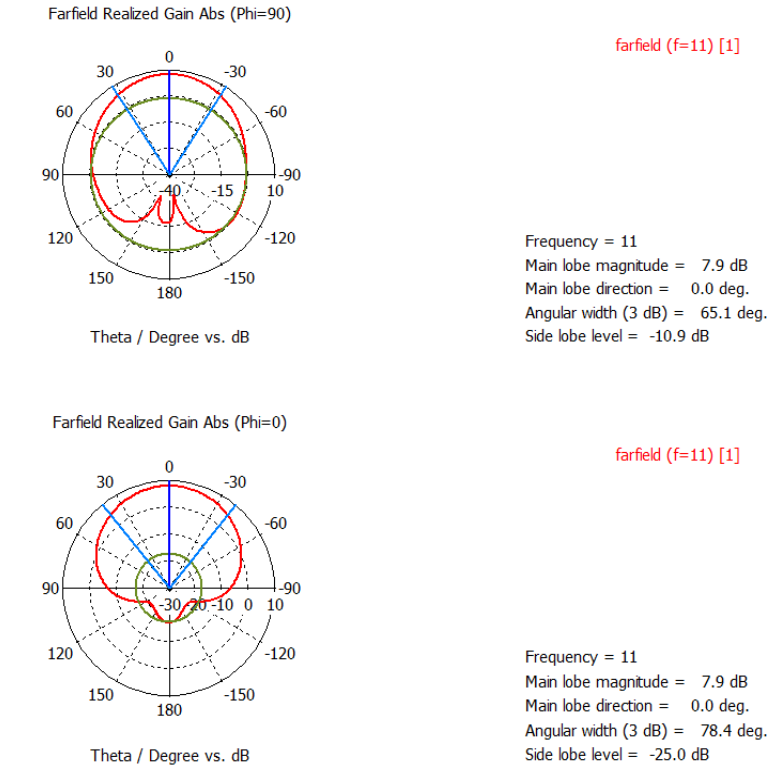

Figure 7. 9: E and H plane radiation pattern of cylindrical shape DRA

Figure 7.10 and 7.11 shows the maximum realized gain achieved by the rectangular and cylindrical shape DRA respectively. Both the antenna gives the average gain above 6 dBi

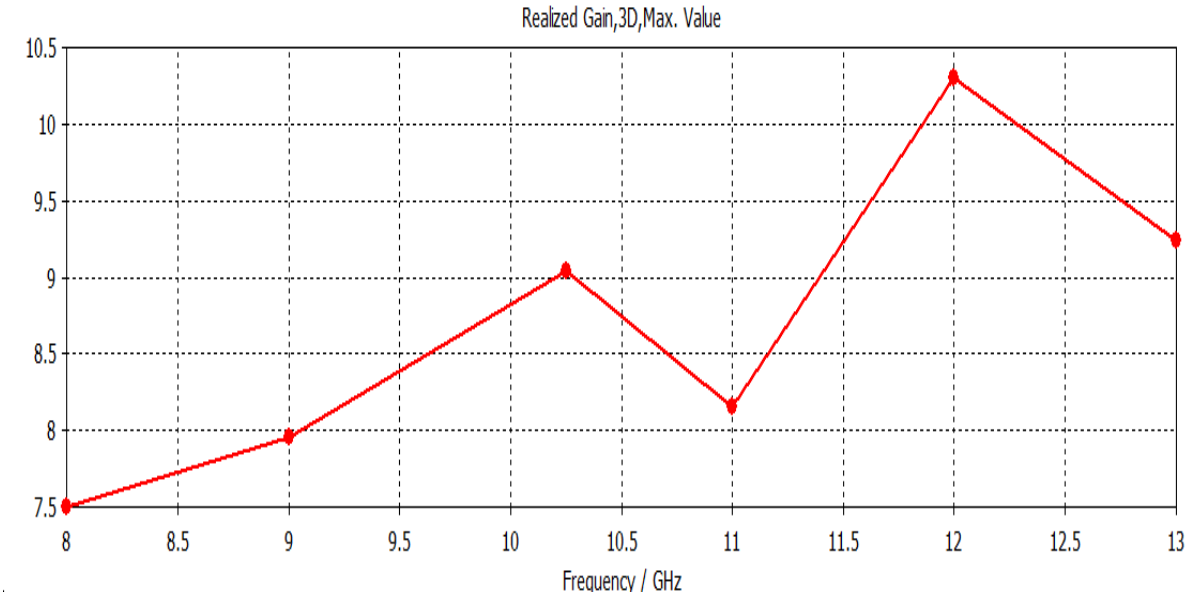

Figure 7.10 Maximum Realized gain of rectangular shape DRA

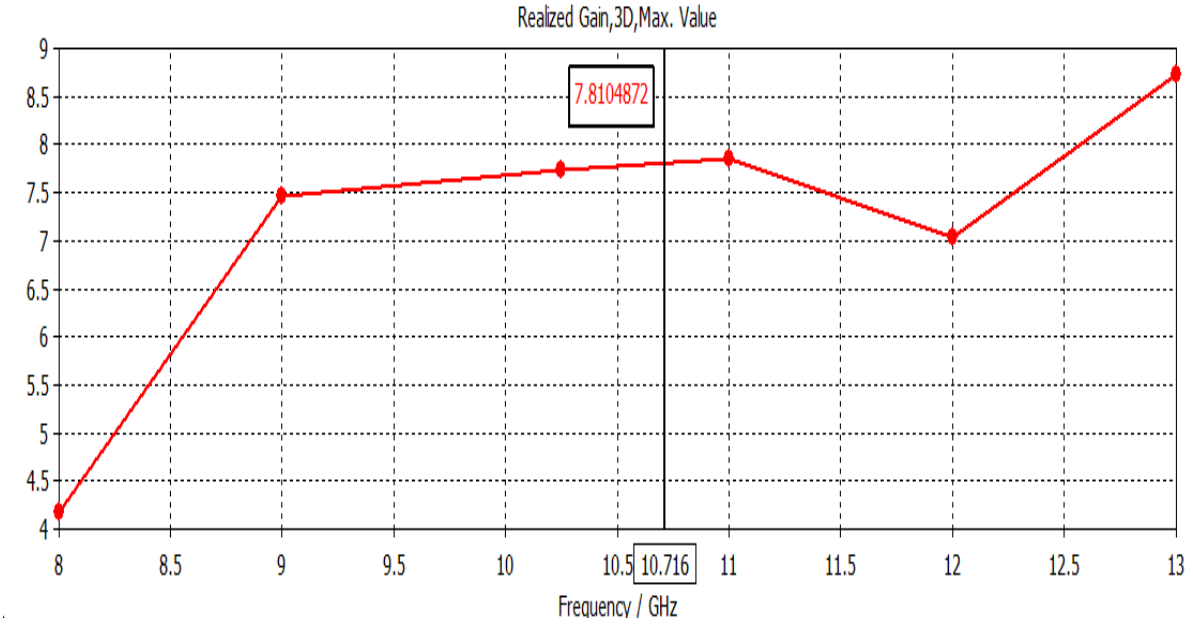

Figure 7.11 Maximum Realized gain of cylindrical shape DRA

Chapter 8

Conclusion

The design equations for predicting the resonant frequency and radiation Q-factor for isolated hemispherical, Cylindrical and Rectangular DRA give good result with little error. The design in chapter 6 i.e. the aperture coupled hemispherical DRA validate the design equations where the simulated resonant frequency of 5.17 GHz and bandwidth of 7.7% is obtained which is very close to the predicted value of 5.2 GHz and 8% respectively. The gain of this basic DRA is found to be 5.7dBi.The small error in frequency and bandwidth is due to the loading of feeding mechanism used to excite the DRA. Thus, the design equations can be very helpful for antenna designer while making initial design with required resonant frequency and bandwidth.

The excitation of various modes in DRA depends on the type of feed and its location w.r.t. the DRA. For any fixed mode in DRA, the resonant frequency and bandwidth can be tuned by slightly changing length and location of the feed. An optimal length and location of the feed can thus be determined for the required resonant frequency and bandwidth. Various bandwidth enhancement techniques covered in the thesis can be used to obtain dual band or wide band operation. The three designs at the end of the thesis shows that the DRA can be combined with other classes of antennas like monopole patch or can be modified in shapes to enhance the bandwidth. Thus DRA is versatile, flexible in design. It has high gain and bandwidth as compared to patch antenna. Moreover, it has no conduction loss. The above mentioned characteristics make DRA a potential candidate to be used in compact portable wireless devices, military millimetre-wave radar equipment and satellite communication.

.

Bibliography

[1] Richtinger R.D., "Dielectric Resonators", *Journal of Applied Physics*, Vol. 10, June 1939, pp. 391-398.

[2] Okaya A., and L.F.Barash,"The Dielectric Microwave Resonator", *Proceedings of the IRE*, Vol. 50, Oct. 1962, pp. 2081-2092.

[3] Cobin S.B., "Microwave Bandpass Filters Containing High Q Dielectric Resonators", *IEEE Transactions on Microwave Theory and Techniques*, Vol. 16, April 1968, pp. 218-227.

[4] Fiedziuszko S.J., "Microwave Dielectric Resonators", *Microwave Journal*, Sept. 1986, pp. 189-200.

[5] Long S.A., M.W. McAllister, and L.C. Shen, "The Resonant Cylindrical Dielectric Cavity Antenna", *IEEE Transactions on Antennas and Propagations*, Vol. 31, No. 3, March 1983, pp. 406-412.

[6] M.W. McAllister, and S.A Long, "Rectangular Dielectric Resonator Antenna", *IEEE Electronics Letters*, Vol. 19, March 1983, pp. 218-219.

[7] M.W. McAllister, and S.A Long, "Resonant Hemispherical Dielectric Antenna", *IEEE Electronics Letters*, Vol. 20, Aug 1984, pp. 657-659

[8] Mongia R.K., and P. Bhartia, "Dielectric Resonator Antennas – A Review and General Design Relations for Resonant Frequency and bandwidth", *International Journal of Microwave and Millimeter-Wave Computer-Aided Engineering*, Vol. 3, June 1998, pp. 35-48

[9] Constantine A. Balanis, "Antenna Theory", London, John Wiley and Sons, 2005.

[10] Kwai-Man Luk and Kwoi-Wa Leung, "Dielectric Resonator Antennas",London, Research Studies Press Ltd, 2003.

[11] Petosa Aldo, "Dielectric Resonator Antenna Handbook", London, Artech House, 2007.